

R. Todd Frahm, Esq., OR Bar No. 192320
tfrahm@tylerbursch.com
TYLER & BURSCH, LLP
25026 Las Brisas Road
Murrieta, California 92562
Telephone: (951) 600-2733
Facsimile: (951) 600-4996

Attorneys for Plaintiff **Steven Arthur Latulippe, M.D.**

IN THE UNITED STATES DISTRICT COURT
FOR THE DISTRICT OF OREGON
PORTLAND DIVISION

STEVEN ARTHUR LATULIPPE, M.D.,

Plaintiff,

vs.

KATHLEEN HARDER, in her official capacity as Chair of the Oregon Medical Board; **SAURABH GUPTA**, in her official capacity as Vice Chair of the Oregon Medical Board; **ERIN CRAMER**, in his official capacity as Secretary/Physician Assistant Member of the Oregon Medical Board; **ROBERT M. CAHN**, in his official capacity as a member of the Oregon Medical Board; **JAMES K. LACE**, in his official capacity as a member of the Oregon Medical Board; **CHARLOTTE LIN**, in her official capacity as a member of the Oregon Medical Board; **PATTI LOUIE**, in her official capacity as a member of the Oregon Medical Board; **JENNIFER L. LYONS**, in her official capacity as a

Case No.:

COMPLAINT FOR DECLARATORY AND INJUNCTIVE RELIEF AND DAMAGES

DEMAND FOR JURY TRIAL

1 member of the Oregon Medical Board;
2 **ALI MAGEEHON**, in her official
3 capacity as a member of the Oregon
4 Medical Board; **CHERE PEREIRA**, in
5 her official capacity as a member of the
6 Oregon Medical Board; **CHRISTOFFER**
7 **POULSEN**, in his official capacity as a
8 member of the Oregon Medical Board;
9 **ANDREW SCHINK**, in his official
capacity as a member of the Oregon
Medical Board; **JILL SHAW**, in her
official capacity as a member of the
Oregon Medical Board,

10 Defendants.

11 INTRODUCTION

13 1. The crux of this case is whether the Oregon Medical Board (“OMB”) was
14 justified in denying Doctor Steven LaTulippe adequate due process because he was a
15 danger to the public.

16 2. Dr. LaTulippe, a retired U.S. veteran, is the healthcare provider for South
17 View Medical Arts located in Dallas, Oregon. After 20-plus years of practicing medicine,
18 on December 3, 2020, the OMB suspended Dr. LaTulippe’s license without a hearing
19 because he was not strictly following the Oregon Occupational Safety and Health
20 Administration (OHSA) and Oregon Health Authority (OHA) COVID-19 mask protocols.

21 3. The OMB’s decision established a per se rule that a doctor is a danger to his
22 patients if he or she does not follow the medical guidance of the administrative state, i.e.,
23 unelected government officials.

24 4. In reality though Dr. LaTulippe has harmed no one. His COVID-19 Protocol
25 has been highly successful. No COVID-19 case has been traced to his office.

5. Accordingly, the OMB's arbitrary decision to revoke Dr. LaTulippe's license is not based on law or facts but a mere difference in medical opinion. Indeed, the OMB's medical opinions have been largely disputed by reputable studies and medical experts.

6. The OMB has violated Dr. LaTulippe's rights to due process and speech under the U.S. Constitution.

PARTIES – PLAINTIFFS

7. Plaintiff, STEVEN A. LATULIPPE, is a U.S. Airforce veteran and has served as a doctor in Dallas, Oregon for 20-plus years. He currently resides in West Salem, Oregon.

PARTIES – DEFENDANTS

8. Defendants, at all relevant times, were duly appointed members of the Oregon Medical Board (OMB), which is an agency of the State of Oregon and is authorized to investigate and discipline physicians for certain statutory and regulatory violations.

9. At all material times, Defendants were persons acting under the color of state pursuant to 42 U.S.C. § 1983.

JURISDICTION AND VENUE

10. This civil rights action raises federal questions under the Fourteenth and First Amendments of the United States Constitution, and under federal law, particularly 42 U.S.C. § 1983.

11. This Court has subject matter jurisdiction over the federal claims pursuant to 28 U.S.C. §§ 1331 and 1343.

12. This Court has authority to grant the requested declaratory relief under the Declaratory Judgment Act, 28 U.S.C. §§ 2201 and 2202, implemented through Rule 57 of the Federal Rules of Civil Procedure. This Court is also authorized to grant injunctive relief and damages under 28 U.S.C. § 1343, pursuant to Rule 65 of the Federal Rules of Civil Procedure, and reasonable attorney's fees and costs under 42 U.S.C. § 1988.

13. Venue is proper in this Court under 28 U.S.C. § 1391(b)(1)(2) because all Defendants are situated in this judicial district, and a substantial part of the events or omissions giving rise to Plaintiff's claims occurred in this district.

FACTUAL BACKGROUND

A. Dr. Steven LaTulippe's Background and Training

14. At all relevant times, Dr. LaTulippe possessed the education, training, and clinical experience to practice medicine in the State of Oregon.

15. Dr. LaTulippe is a decorated and well-respected U.S. veteran and Oregon medical provider.

16. On or around 1975, Dr. LaTulippe enlisted in the U.S. Air Force, with a focus in aviation. He had the opportunity to fly the KC-135 Stratotanker and the RF-4C Phantom. He also had the privilege of acting as the Chief of Medical Services, the Medical Review Officer, the Chief of Pharmacy Services and a physician with the Oregon Air National Guard.

17. On or around 1978, Dr. LaTulippe, studied biology with an emphasis on microbiology at Boise State University. After graduating from Boise State, he attended the University of Massachusetts to study microbiology in the PhD program. He also taught general microbiology and bacteriology for one year in the PhD program.

18. On or around 1989, and while flying the RF-4C Phantom in the U.S. Air Force, Dr. LaTulippe attended Boise Bible College and became an ordained minister.

19. On or around 1991, Dr. LaTulippe attended the Cincinnati Bible Seminary.

20. On or around 1993, Dr. LaTulippe enrolled in medical school at Lorma Linda University. Upon graduating in 1997, he completed his residency in rural medicine in Wheeling, West Virginia.

21. On or around 2000, Dr. LaTulippe moved to Dallas, Oregon. He opened up a practice in Dallas (South View Medical Arts) that focused on, and still focuses on, pain and addiction and full-spectrum family medicine. He moved to West Salem in 2013.

1 22. In addition to providing pain and addiction services, Dr. LaTulippe provides
 2 immediate care, gynecology services, dermatologic care, psychiatric care, endoscopies,
 3 and geriatrics.

4 23. Dr. LaTulippe uniquely treats chronic pain—including fibromyalgia, low
 5 back pain, neck pain and joint pain – by prescribing appropriate adjunctive and opioid
 6 therapies focusing on central pain.

7 24. The central pain treatment has been an enormous blessing and revelation to
 8 many of Dr. LaTulippe’s patients.

9 25. Dr. LaTulippe receives referrals from all over Oregon – many of whom come
 10 from underprivileged socio-economic backgrounds.

11 26. On or around the middle of November 2020, Dr. LaTulippe received a
 12 “Certificate of Long-term American Academic of Family Physicians (AAFP)
 13 Achievement.” A true and correct copy of his Certificate is attached hereto as Exhibit “A.”

14 **B. The OMB’s Suspension of Dr. LaTulippe’s License**

15 27. On or around August 13, 2020, the OMB opened an investigation against Dr.
 16 LaTulippe based upon allegations that he was advising the public to not wear a mask,
 17 including posting on social media.

18 28. That same day, Dr. LaTulippe received a phone call from an anonymous man
 19 who said he was going to “take him down.”

20 29. On or around November 7, 2020, Dr. LaTulippe spoke at a “Stop the Steal
 21 Rally” in Salem, Oregon. During the rally, he spoke about the ineffectiveness of masks.

22 30. On or around November 9, 2020, the medical director of the OMB, David
 23 Farris, sent Dr. LaTulippe a letter saying Dr. LaTulippe was in violation of the Governor’s
 24 Executive Orders and the administrative rules issued by OHA, requiring people to wear
 25 properly fitted masks.

26 31. On or around December 2, 2020, an investigator arrived at Dr. LaTulippe’s
 27 office unannounced. The investigator observed the office but never inquired with staff or

1 Dr. LaTulippe about his COVID-19 protocol or ask if any COVID-19 cases were traced
2 to the office.

3 32. On or around December 3, 2020, Jason Carruth, a purported investigator with
4 the OMB, called Dr. LaTulippe to inform him the OMB suspended his license.

5 33. Shortly after the call, Dr. LaTulippe read about his suspension on the news.

6 34. On or around December 5, 2020, Dr. LaTulippe was served with the
7 suspension letter and “Order of Emergency Suspension of License.” A true and correct
8 copy of the Order is attached hereto as Exhibit “B.”

9 35. The OMB relied on Oregon Revised Statutes (ORS) 677.205(3) and
10 183.430(2), to circumvent procedural due process and thereby deny Dr. LaTulippe a
11 hearing.

12 36. ORS 677.205(3) allows the OMB to temporarily suspend a license without a
13 hearing if there is evidence that a licensee’s continued practice constitutes an immediate
14 danger to the public.

15 37. ORS 183.430(2) allows a temporary suspension if the board has found that a
16 licensee’s continued practice of medicine by a physician presents a serious danger to the
17 public health or safety.

18 38. ORS 677.205(3) and ORS 183.430(2) requires different procedures. The
19 OMB did not clarify which procedure it intends to follow.

20 39. The board found that Dr. LaTulippe presented a serious danger to the public
21 health and safety. This conclusion was based upon “sources that are well recognized in
22 the medical community” and complaints submitted by an unknown party (patient A) and
23 a private investigator.

24 40. According to the OMB, OHA and OSHA, public health and safety requires
25 health care practitioners to wear masks and require patients and staff to wear masks in the
26 clinical setting. Health care providers must also adopt, enforce, and post COVID-19
27 transmission prevention policies and protocols.

1 41. The OMB stated, in its finding of facts, that patient A claimed Dr. LaTulippe
 2 directed him or her not to self-isolate because they should be around others to build
 3 COVID-19 immunity.

4 42. The OMB also found that Dr. LaTulippe and his staff refused to wear a mask
 5 in the clinic, urged people to remove their mask when they enter the clinic, and provided
 6 no hand sanitizer or screening protocol.

7 **C. Dr. LaTulippe's COVID-19 Practices, Protocols, and Results**

8 43. Since the inception of COVID-19, Dr. LaTulippe has followed a strict
 9 COVID-19 protocol, which is posted throughout his office. A true and correct copy of the
 10 COVID-19 Protocol is attached hereto as exhibit "C."

11 44. On the lobby door is a sign that reads, "Our office is following Corona Virus
 12 (COVID-19) protocol. We appreciate your cooperation and understanding during this
 13 confusing time." A true and correct copy of the sign is attached hereto as Exhibit "D."

14 45. Dr. LaTulippe's protocol requires all patients stay six feet apart. Most the
 15 time, there was only one patient in the lobby.

16 46. Dr. LaTulippe's practice only has two staff members, one being his wife.

17 47. Dr. LaTulippe and his staff ensures there are no crossing of paths amongst
 18 patients. All patients are directed in a one-way circle around the office.

19 48. All patients and staff are required to wash their hands before and after each
 20 patient contact. Staff also wear gloves and sterilize and disinfect the treatment rooms after
 21 patient use.

22 49. Whenever a patient expresses or exhibits COVID-19 symptoms such as a
 23 fever, diarrhea, coughing, congestion, tightness in chest, shortness of breath, muscle
 24 tightness, or fatigue, the patient is required to wear a mask while visiting the clinic.

25 50. If a patient calls and expresses COVID-19 symptoms, he or she is instructed
 26 to visit the clinic at the end of business hours, when there are no other patients in the lobby.

1 51. When a patient with COVID-19 symptoms arrives at the office, there are no
2 other patients in the waiting room. The patient is directed to a designated room reserved
3 for COVID-19 treatment.

4 52. Once a COVID-19 patient exits the office, staff disinfect and sterilize the
5 designated COVID-19 room for future appointments.

6 53. Dr. LaTulippe treats COVID-19 patients with Prednisone, Symbicort,
7 Ventolin, Azithromycin, and Doxycycline. If a patient has GI symptoms, a headache, and
8 myalgias (flu-like symptoms), they are treated with Pedialyte. A true and correct copy of
9 the COVID-19 Treatment Protocol is attached hereto as Exhibit "E."

10 54. Dr. LaTulippe has never told a patient they cannot wear a mask in his office.
11 He provides all patients with COVID-19 related information so they can make an informed
12 decision.

13 55. He has treated approximately 200 patients who have experienced physical
14 manifestations from wearing a mask like fainting, dizziness, migraines, asthma, allergies,
15 pneumonia, COPD exacerbations, nasal postal osis, parotitis, pink eye, sinusitis, and oral
16 gingivitis. He advises these patients to not wear a mask as much as possible and to avoid
17 places where they would be forced to wear a mask.

18 56. Dr. LaTulippe provides hand sanitizer at the front desk near the receptionist
19 so no one steals it.

20 57. There has been no reported person to person COVID-19 infections traced to
21 Dr. LaTulippe's office, and none of his staff have contracted the disease.

22 58. All of Dr. LaTulippe's patients with COVID-19 symptoms have experienced
23 improvement from the symptoms.

24 **D. The Effectiveness of Masks in Combatting COVID-19 Has Been Disputed**

25 59. Because most of the allegations of the investigator are untrue, the remaining
26 essence of OMB's decision to suspend Dr. LaTulippe's medical license is that he and his
27

1 staff do not wear a mask in the medical office and that he stated his political views on this
 2 subject clear at a political rally.

3 60. Medical experts and reputable studies reveal that masks are ineffective at
 4 curtailing the spread of COVID-19.

5 61. For instance, a Danish study conducted by ACP Journals during April 2 to
 6 June 2, 2020 – a period when Danish authorities did not recommend mask use – found
 7 that a recommendation to wear a surgical mask did not reduce, “at conventional levels of
 8 statistical significance, incident SARS-CoV-2 infection compared with no mask
 9 recommendation.”¹ A true and correct copy of the Danish study is attached hereto as
 10 Exhibit “F.”

11 62. Further, masks are ineffective viral barriers because the particles of COVID-
 12 19 are small enough to enter through the surface of a cloth mask. Particles from wildfire
 13 smoke are between .4 and .7 microns and COVID-19 is between .1 and .5 microns.² A true
 14 and correct picture of a COVID-19 particle is attached hereto as Exhibit “G.”

15 63. In a study conducted in Physics of Fluids, by AIP Publishing, researchers
 16 from the University of Massachusetts Lowell and California Baptist found that wearing a
 17 mask does not prevent particles smaller than 2.5 micrometers from spreading.³ A true and
 18 correct copy of this study is attached hereto as Exhibit “H.”

19 64. Because masks are not effective in slowing the spread of COVID-19, Dr.
 20 LaTulippe only requires patients who are symptomatic to wear masks in his clinic.

21 65. Further, Dr. LaTulippe’s staff do not wear masks because they experience
 22 shortness of breath, claustrophobia, and panic attacks.

23
 24 ¹ Available as of the date of filing: <https://www.acpjournals.org/doi/full/10.7326/M20-6817>

25 ² Available as of the date of filing: <https://www.visualcapitalist.com/visualizing-relative-size-of-particles/>. For example, masks do not prevent the smell of cigarette smoke from passing through a
 26 mask.

27 ³ <https://aip.scitation.org/doi/10.1063/5.0034580>

E. Dr. LaTulippe's Continued Suspension Will Lead to Irreparable Harm

66. Since Dr. LaTulippe's suspension, many of his patients have suffered greatly.

67. For many patients, Dr. LaTulippe is their only doctor. They rely primarily on him to receive consequential treatment and prescriptions. Without his services, they are suffering extreme pain and anxiety.

68. Dr. LaTulippe is the only doctor within reasonable driving distance of Dallas, Oregon that specializes in pain and addiction.

69. Approximately one-half of Dr. LaTulippe's patients visit him for pain and addiction treatment because he specializes in central pain medicine, which is a unique specialty.

70. Central pain is commonly mistreated with opioids, which does not cure pain symptoms and can lead to addiction.

71. A significant number of patients were referred to Dr. LaTulippe after they failed opioid treatment elsewhere.

72. His treatment has assisted their pain and allowed them to control their addictions, and they will find it extremely hard, if not impossible, to find another doctor within a reasonable driving distance that can replace him.

FIRST CAUSE OF ACTION

The OMB Violated the Due Process Clause of the Fourteenth Amendment to the U.S. Constitution

73. Dr. LaTulippe realleges and incorporates by reference the paragraphs above.

74. 42 U.S.C. § 1983 provides that a party shall be liable when it “subjects, or causes to be subjected, any person of the United States or other person within the jurisdiction thereof to the deprivation of any rights, privileges, or immunities secured by the Constitution and laws of the United States.”

75. Dr. LaTulippe was not afforded adequate due process before his property (his medical license) was taken from him.

76. Defendants willfully deprived and violated Dr. LaTulippe's procedural due process rights by:

(a) Relying on ORS 677.205(3) and 183.430(2) to interfere with and impede Dr. LaTulippe's ability to practice medicine.

(b) Failing to provide Dr. LaTulippe with a hearing before his suspension under the pretext that he posed an imminent danger to the public's health or safety.

(c) Failing to make clear which procedure it intends to follow and thereby impairing Dr. LaTulippe's ability to pursue a defense.

(d) Failing to articulate which laws Dr. LaTulippe has actually violated.

(e) Suspending Dr. LaTulippe's license without first issuing or serving an emergency order prior to the suspension as required by OAR 137-003-0560.

77. As a result of Defendants' conduct, Dr. LaTulippe has suffered economic damages for the loss of wages and impairment of his earning capacity in an amount to be determined at trial.

78. Dr. LaTulippe has also suffered noneconomic damages for mental and emotional distress and loss to his reputation in an amount to be determined at trial.

SECOND CAUSE OF ACTION

The OMB Violated the Speech Clause of the First Amendment to the U.S. Constitution

79. Dr. LaTulippe realleges and incorporates by reference the paragraphs above.

80. The OMB's suspension of Dr. LaTulippe was based on the fact he has publicly stated at a political rally ("Stop the Steal" rally) that masks are not effective in slowing the spread of COVID-19.

81. In context, the statements we made at a Stop the Steal Rally to a politically driven group of people sympathetic to assertions that there was election fraud and who were opposed to COVID-19 lockdowns. The statements were intended to rally a political view against COVID-19 lockdowns, against COVID-19 policies restricting freedom of

expression, speech, and liberty, and to encourage people to favor President Donald Trump as an alternative to the lockdowns generally occurring in Democrat controlled states.

3 82. Dr. LaTulippe's speech was among numerous other politically driven
4 speeches, was expressed within a political gathering, and was expressed as part of a larger
5 overall message intended by its organizers to arose support for President Trump.

6 83. The OMB's suspension targeted Dr. LaTulippe because he spoke at a rally
7 supporting President Trump and against certain COVID-19 policies.

8 84. The OMB's suspension is also based upon public comments Dr. LaTulippe
9 has made to his patients.

10 85. Even though Dr. LaTulippe made comments in public about masks, he never
11 prevented any patient from wearing a mask in the office. Furthermore, Dr. LaTulippe
12 never told any individual patient to remove their mask for any reason other than medical
13 necessity.

14 86. The OMB's suspension restrains verbal as well as the non-verbal expressive
15 conduct of refusing to wear a mask.

16 87. The restraint of Dr. LaTulippe's speech is not justified by strict scrutiny.

17 88. As a result of Defendants' suspension, Dr. LaTulippe has suffered economic
18 damages for the loss of wages of his earning capacity in an amount to be determined at
19 trial.

20 89. Dr. LaTulippe has also suffered noneconomic damages for mental and
21 emotional distress and loss to his reputation in an amount to be determined at trial.

PRAYER FOR RELIEF

WHEREFORE, Plaintiffs pray for relief as follows:

24 1. That this Court enter a Declaratory Judgment declaring Defendants'
25 suspension of Dr. LaTulippe's license violated his procedural due process rights;

26 2. That this Court enter a Declaratory Judgment declaring Defendants' conduct
27 violated Dr. LaTulippe's First Amendment rights;

3. That this Court issue a temporary, preliminary, and permanent injunction enjoining the OMB's suspension of Dr. LaTulippe's license and thereby reinstating his license;

4. That this Court award Dr LaTulippe compensatory and general damages in
an amount according to proof;

5. That this Court award Dr. LaTulippe special damages in an amount according to proof;

6. That this Court award Dr. LaTulippe punitive damages;

7. That this Court declare Dr. LaTulippe the prevailing party and award him the reasonable costs and expenses of this action, including reasonable attorney's fees in accordance with 42 U.S.C. §1988; and

8. That this Court grant such other and further relief as this Court deems equitable and just under the circumstances.

Respectfully submitted,

TYLER & BURSCH, LLP

Dated: January 20, 2021

/s/ R. Todd Frahm
R. Todd Frahm
Attorney for Plaintiff **Steven Arthur Latulippe, M.D.**

EXHIBIT A



Steven A LaTulippe, MD

is recognized with this

Certificate of Long-term AAFP Membership

The AAFP is indeed grateful to its long-term members for their role in helping establish the specialty of family medicine, for maintaining the high standards and principles of medicine, and for their commitment to continuing, comprehensive quality care for the American public.

Executive Vice President

A handwritten signature in black ink, appearing to read "R. John Ryland".

25 years

EXHIBIT B



Oregon

Kate Brown, Governor

December 4, 2020

Medical Board
1500 SW 1st Avenue, Suite 620
Portland, OR 97201
(971) 673-2700
FAX (971) 673-2670
www.oregon.gov/omb

SENT VIA CERTIFIED RETURN RECEIPT MAIL

Article No. 7020 1810 0000 4068 9790

Steven Arthur LaTulippe, MD
PO Box 787
531 SE Clay St
Dallas, OR 97338

RE: Order of Emergency Suspension

Dear Dr. LaTulippe:

Enclosed is a copy of the Order of Emergency Suspension which was approved by the Oregon Medical Board on December 3, 2020.

If you have any questions or concerns regarding this Order, please contact me or Jason Carruth, Investigator at (971) 673-2700.

You may be required to report this Order to other state boards or entities. It is your responsibility to know the rules and regulations as they relate to the reporting of this Oregon action. The Board recognizes that other state boards may choose to take action based on the Oregon action. You are reminded that you are obliged to report any official action taken against you to the Board within 10 working days. "Official action" is defined in Oregon Revised Statute 677.415(b) as, "a restriction, limitation, loss or denial of privileges of a licensee to practice medicine, or any formal action taken against a licensee by a government agency or a health care facility based on a finding of medical incompetence, unprofessional conduct, physical incapacity or impairment." When reporting an official action to the Board, please include a copy of the action with your report.

Sincerely,

A handwritten signature in black ink, appearing to read "Eric Brown".

Eric Brown
Chief Investigator
Investigations/Compliance Unit

EB:ms
Enclosures

cc: Warren Foote, JD/Katharine DisSalle, JD, Board Counsel, *via electronic transmission*



BEFORE THE
OREGON MEDICAL BOARD
STATE OF OREGON

In the Matter of)
STEVEN ARTHUR LaTULIPPE, MD) ORDER OF EMERGENCY
LICENSE NO. MD22341, Licensee) SUSPENSION OF LICENSE AND
) NOTICE OF OPPORTUNITY FOR
) HEARING

By order of the Oregon Medical Board, the license of Steven A. LaTulippe, MD to practice medicine is hereby suspended, effective December 3, 2020, at 5:15 p.m. Pacific Time. As of this date and time, Licensee must stop practicing medicine until further order of the Board.

1.

AUTHORITY

1.1 The Oregon Medical Board (Board) is the state agency responsible for licensing, regulating and disciplining certain health care providers, including physicians, in the State of Oregon. Under ORS chapter 677, the Board has the duty to protect the public and to exercise general supervision over the practice of medicine. Steven Arthur LaTulippe, MD (Licensee) is a licensed physician in the State of Oregon.

1.2 This order is made pursuant to 677.205(3), which authorizes the Board to temporarily suspend a license without a hearing when the Board has evidence that indicates that Licensee's continued practice constitutes an immediate danger to the public, as well as ORS 183.430(2), in that the Board has found that Licensee's continued practice of medicine by a physician presents a serious danger to the public health or safety.

2.

When making determinations about public health and safety, the Board relies upon sources that are well recognized in the medical community and are relied upon by physicians in

their delivery of care to patients. For this case, the Board relies upon basic principles of transmission of respiratory viruses and of respiratory physiology, as well as formal SARS-CoV-2 (COVID-19) guidelines published by the Oregon Health Authority (OHA), and the corresponding rules for workplace safety promulgated by the Oregon Safety and Health Administration (OSHA).

3.

7 3.1 The spread of COVID-19 is a global pandemic. While most people only
8 experience mild symptoms from COVID-19, some become severely ill and die from the
9 infection. COVID-19 is highly contagious. There are medications that help patients with severe
10 illness but there is no effective treatment at this time.

11 3.2 COVID-19 is spread from symptomatic and asymptomatic people primarily
12 through respiratory droplets expelled when an infected person talks, coughs, or sneezes. These
13 droplets infect others through contact with moist surfaces in one's nose, mouth, throat, eyes or
14 lungs. Infection most commonly happens when people are near each other – within six feet.
15 COVID-19 can also be transmitted when one touches an object with virus present and then
16 touches one's own mouth, eyes, or nose. Although masks vary in effectiveness, even the simplest
17 mask can be expected to contain the largest, most infectious droplets. The effectiveness of masks
18 has been scientifically shown to decrease disease transmission in the current pandemic.

19 3.3 When infected with COVID-19 patients can have a wide range of symptoms.
20 Infected persons often experience no symptoms at all or have very mild symptoms resembling a
21 cold or flu. Others experience severe symptoms that require hospitalization, medication and
22 sometimes placement on a ventilator. Most of those who develop severe, life-threatening
23 symptoms are older and have underlying health conditions. However, there have been cases of
24 children and young, otherwise healthy, adults who have experienced severe disease and required
25 hospitalization.

26 3.4 Every member of the public is at risk – this virus is easily transmitted from person
27 to person. It has even been shown to be transmitted by individuals with few or no symptoms. The

1 elderly, those with chronic health conditions, those living in group care settings, and health care
 2 workers are particularly at risk for developing life threatening illness. Steps to protect oneself
 3 and others include: Covering the nose and mouth by wearing a mask when in public, washing or
 4 sanitizing hands frequently, remaining at least six feet away from people outside of one's
 5 household, avoiding crowds, staying home and away from others if sick, elderly, or have
 6 underlying medical conditions.

7 3.5 As OHA and OSHA have set forth, public health and safety requires health care
 8 practitioners to wear masks and require patients and staff to wear masks in the clinical setting.
 9 Health care providers must also adopt, enforce, and post COVID-19 transmission prevention
 10 policies and protocols.¹

11 ¹ OHA has promulgated guidance in health care settings. OSHA administrative rules OAR 437-001-0744 and
 12 Appendices require all employers to follow OHA guidance on COVID-19. OHA Guidance includes but is not
 limited to:

13 Effective July 20, 2020 – All health care clinics must: have and enforce policies that require all individuals who
 enter the health care office to wear a face mask, face covering or face shield while inside, including when in a
 14 private examination room, except as follows: If a patient cannot tolerate any form of face mask, face covering or
 face shield due to a medical condition, strict physical distancing must be observed until the patient can be placed or
 15 roomed in an area that minimizes risk to others. A face mask, face covering or face shield is not required to be worn
 during an examination or procedure in which access to parts of the face that are covered by a face mask, face
 covering or face shield is necessary. A face mask, face covering or face shield is required to be worn as soon as the
 16 examination or procedure in question has completed; have and enforce policies that require health care personnel to
 wear appropriate personal protective equipment (PPE) for the care of patients with suspected COVID-19, confirmed
 17 COVID-19, or a known exposure to COVID-19. All health care providers must: Wear a face mask or face covering
 that covers the nose and mouth at all times while in the health care office, except when in a private office by
 18 themselves; face masks should be prioritized over face coverings because they offer both source control and
 protection for the health care provider from potentially infectious droplets, splashes, or sprays; cloth face coverings
 19 may not be worn instead of a respirator or face mask if more than source control is needed; health care providers
 should avoid touching the outside (contaminated) surface of a face mask or face covering. If a health care provider
 20 must adjust the face mask or face covering, hand hygiene should be performed immediately after adjustment; face
 shields should be worn in addition to, but not in place of, face masks for the purposes of eye protection and
 21 additional layer of splash protection; face masks or face coverings are not required while eating or drinking, but
 strict physical distancing should be maintained while face masks, face shields, or face covering are not worn; health
 22 care providers must wear N95 masks or higher-level respiratory protection instead of a face covering or face masks
 for patient care that warrants a higher level of protection (See “PPE for Healthcare Personnel” Section); respirators
 23 with exhalation valves may not be worn. Patients and visitors: All patients and visitors when visiting a health care
 office are required to wear a face mask, face covering, or face shield unless the individual is under five (5) years of
 24 age, except as follows: Face masks, face shields or face coverings are not required while eating or drinking, but
 strict physical distancing (6 feet or more) should be maintained while face masks, face shields, or face covering are
 25 not worn; a face mask, face covering or face shield is not required to be worn during an examination or procedure
 where access to parts of the face that are covered by a face mask, face covering or face shield is necessary; a face
 26 mask, face covering or face shield is required to be worn as soon as the examination or procedure in question has
 completed; face masks, face shields or face coverings can be briefly removed in situations where identity needs to be
 27 confirmed by visual comparison; if possible, limit speaking while the cover is off as speaking generates aerosols and
 droplets that can contain viruses; it is not recommended that individuals wear a face shield instead of a face mask or
 face covering - face shields provide protection for the eyes and additional layer of splash or spray protection, but the

1 3.6 Under basic principles of respiratory physiology, the body reflexively maintains
 2 carbon dioxide content within narrow parameters, by adjusting the minute ventilation (the
 3 volume of gas inhaled and exhaled in 60 seconds). The amount of carbon dioxide re-breathed
 4 within a mask is trivial and would easily be expelled by an increase in minute ventilation so
 5 small it would not be noticed. Although patients with extremely advanced lung disease may not
 6 be able to increase their minute ventilation, their pre-existing metabolic compensation would
 7 readily address the trivial potential increase in carbon dioxide content.

8

9 role of face shields as a method of source control has not been established; use of a face shield alone should be
 10 limited to situations when wearing a face mask or face covering is not feasible in the following situations: when a person has a medical condition that prevents them from wearing a face mask or face covering; when people need to see mouth and tongue motions in order to communicate (e.g., when communicating with people with hearing impairments).

11 Effective July 31, 2020: An office must implement strict infection controls in accordance with following OHA
 12 guidance: Symptoms of COVID-19 include fever, cough, shortness of breath, fatigue, myalgia, and headache. Less
 13 common symptoms include sore throat, diarrhea, and loss of smell and taste. Fever is likely during the clinical
 14 course, but some data indicate that fewer than half of hospitalized COVID-19 patients present with fever. Severity of
 15 illness may worsen in the second week of infection. Atypical presentations have been described in older adults and
 16 persons with comorbidities. CDC has provided details on the clinical presentation of COVID-19. RNA from the
 17 virus that causes COVID-19 (SARS-CoV-2) has been identified from patients who never develop symptoms
 (asymptomatic) and in patients before symptoms develop (presymptomatic). Transmission during both the
 18 asymptomatic and the pre-symptomatic period has been documented. The degree to which pre-symptomatic and
 19 asymptomatic transmission have contributed to the COVID-19 pandemic remains unclear. SARS-CoV-2 is believed
 20 to spread mainly between people in close contact or through respiratory droplets produced by coughs and sneezes.
 21 The virus can survive on surfaces for hours to days but can be rendered inactive by routine cleaning and disinfection
 22 procedures. (See "Environmental Infection Control in Healthcare Setting" Section.)

23 Effective 11/13/2020: Source control (i.e. universal masking) for patients and visitors. Healthcare facilities shall
 24 have policies in place requiring all individuals who enter the facility to don a face covering or face mask while in the building. If a face covering or face mask is not available or is not tolerated by a patient, face shields can also be utilized. If a patient cannot tolerate any form of face covering due to a medical condition, strict physical distancing must be observed until the patient can be placed or roomed in an area that minimizes risk to others. • Source control (i.e. universal masking) for health care personnel. Health care personnel shall wear a face covering or face mask at all times while they are in the healthcare facility. Medical-grade face masks should be prioritized for health care personnel, as they offer both source control and protection for the health care personnel from potentially infectious droplets, splashes, or sprays. Cloth face coverings should not be worn instead of a respirator or face mask if more than source control is needed. Health Care Personnel shall ensure that the mask covers their nose and mouth at all times. Health care personnel should avoid touching the outside (contaminated) surface of the mask. If Health Care Personnel must adjust the mask, hand hygiene should be performed immediately after adjustment. N95s or higher-level respiratory protection should replace face masks for patient care that warrants a higher level of protection. Respirators with exhalation valves are not recommended for source control. Universal eye protection for health care personnel. Wearing eye protection in addition to face mask or an N95 respirator ensures the eyes, nose, and mouth are all protected from exposure to respiratory secretions during encounters in healthcare settings. Due to the increased risk of spread in long-term care settings and the likelihood for close-contact exposures to residents and coworkers, long-term care facility staff should wear a face mask and eye protection (goggles or face shield) at all times within the facility (See "Extended Use of Personal Protective Equipment" Section). Health care personnel in other settings should consider the addition of eye protection to universal masking, particularly in scenarios where patients are unable to wear a face covering. Universal use of PPE does not eliminate the need for physical distancing among health care personnel in the workplace.

1 3.7 Licensee treats Oregon Health Plan (OHP) patients who have limited resources
2 and limited or no ability to transfer their care to another provider.

4.

FINDINGS OF FACT

5 The Board finds Licensee engaged in unprofessional conduct or dishonorable conduct, as
6 defined in ORS 677.188(4)(a), as conduct that is contrary to medical ethics and does or might
7 constitute a danger to the health or safety of the public and committed multiple acts of
8 negligence and gross negligence in the practice of medicine as follows:

9 4.1 On or about July 02, 2020, Patient A – a member of the OHP – contacted
10 Licensee’s medical clinic to request guidance on when and if to be tested for COVID-19. Patient
11 A was told asymptomatic persons should not be tested, that wearing masks does not prevent
12 transmission of COVID-19, and was directed not to self-isolate because being around other
13 people would provide Patient A with immunity to COVID-19. On or about July 23, 2020, after
14 Patient A had questioned the appropriateness of the COVID-19 advice provided, Patient A was
15 terminated as a patient.

16 4.2 Licensee and the staff in his clinic refuse to wear masks in the clinic and urge
17 persons who enter the clinic wearing masks to remove their masks.

18 4.3 Licensee regularly tells his patients that masks are ineffective in preventing the
19 spread of COVID-19 and should not be worn. Licensee further asserts that, because virus
20 particles are so small, they will pass through the recommended N95 masks and most other face
21 coverings people are choosing to wear. Licensee directs patients to a YouTube video providing
22 false information about mask wearing.

23 4.4 Licensee regularly advises, particularly for his elderly and pediatric patients, that
24 it is “very dangerous” to wear masks because masks exacerbate COPD and asthma and cause or
25 contribute to multiple serious health conditions, including but not limited to heart attacks,
26 strokes, collapsed lungs, MRSA, pneumonia, and hypertension. Licensee asserts masks are likely
27 ///

1 to harm patients by increasing the body's carbon dioxide content through rebreathing of gas
2 trapped behind a mask.

3 4.5 Licensee's COVID-19 protocols for his clinic call for patients to be masked only
4 if they present with cough, fever, or "suspicious" viral illness and do not call for any of the
5 health care providers to wear masks unless these conditions exist.

6 4.6 Signage posted in Licensee's clinic asserts the clinic is complying with
7 (unspecified) COVID-19 protocols, but does not include any information on what those
8 protocols are.

9 4.7 On December 2, 2020, a Board investigator visited Licensee's clinic and
10 observed: neither patients nor health providers were wearing masks; no screening procedures
11 were in place or being conducted (e.g., taking patient temperatures on or before entering the
12 clinic); no hand sanitizer was available in the waiting area; a sign was posted in the public area
13 of the clinic with "warning signs" of CO₂ toxicity; an article was posted in the public area of the
14 clinic, with a portion of the article highlighted that claims 94% of the individuals who will
15 experience serious effects of COVID-19 have co-morbidities.

5

CONCLUSIONS OF LAW

18 The Board finds Licensee's continued practice constitutes an immediate danger to the
19 public, and presents a serious danger to the public health and safety as follows:

20 5.1 During the pandemic, patients will inevitably present to Licensee's clinic with
21 known, suspected, or occult infection with SARS-CoV-2; and

22 5.2 Such patients present a clear and present health risk to other patients and staff;
23 and

24 5.3 Licensee's active discouragement of mask wearing by patients and elimination of
25 mask wearing by staff and Licensee represent a failure to take appropriate steps to reduce the risk
26 of transmission, thereby posing an unnecessary and preventable risk to patients, staff, and
27 Licensee; and

5.4. Licensee's instruction and example to patients to shun masks actively promotes transmission of the virus within the extended community; and

5.5 Licensee's advice to patients regarding the failure of masks to prevent viral transmission and potential patient harm due to masks, are counter to basic principles of epidemiology and physiology and undermine acceptability among Licensee's patients and the general populace of one of the primary measures known to significantly diminish viral transmission; and

5.6 Licensee's OHP patients are assigned to physicians by OHP and, if assigned to Licensee, have limited ability to transfer their care to a different provider. These particularly vulnerable patients are, therefore, largely forced to endure Licensee's unsafe practices while his medical license remains active.

6.

NOTICE OF RIGHTS

Licensee has a right to a formal hearing to contest this suspension order. To have a hearing, Licensee must request one in writing. If requested, the hearing will be held pursuant to ORS chapter 183. Licensee has the right to demand the hearing be held as soon as practicable after the Board receives the written request. The written request for hearing must be received within 90 days from the date this order is served on Licensee personally or mailed by certified mail. Licensee will be notified of the time, place and date of hearing. Failure by Licensee to timely request a hearing, failure to appear at any hearing scheduled by the Board, withdrawal of the request for hearing, or failure to appear at any hearing scheduled by the Board on time will constitute waiver of the right to a contested case hearing. In that event, the record of proceeding to date, including Licensee's file with the Board and any information on the subject of the contested case, automatically becomes a part of the contested case record for the purpose of proving a prima facie case per 183.417(4) and this emergency suspension order.

11

111

7.

NOTICE TO ACTIVE DUTY SERVICEMEMBERS: Active duty Servicemembers have a right to stay these proceedings under the federal Servicemembers Civil Relief Act. For more information contact the Oregon State Bar at 800-452-8260, the Oregon Military Department at 503-584-3571 or the nearest United States Armed Forces Legal Assistance Office through <http://legalassistance.law.af.mil>. The Oregon Military Department does not have a toll-free telephone number.

IT IS SO ORDERED THIS 4th day of December, 2020.

OREGON MEDICAL BOARD

State of Oregon

**KATHLEEN M. HARDER, MD
BOARD CHAIR**

1
2
3
4

CERTIFICATE OF MAILING

5 On December 4, 2020, I mailed the foregoing Order of Emergency Suspension regarding Steven
6 Arthur LaTulippe, MD, to the following parties:

By: First Class Certified/Return Receipt U.S. Mail & First Class Mail
Certified Mail Receipt # 7020 1810 0000 4068 9790

9 Steven Arthur LaTulippe, MD
10 PO Box 787
11 531 SE Clay St
12 Dallas, OR 97338

12 By: Secure Electronic Transmission

14 Warren Foote/Katharine Disalle
Department of Justice
15 1162 Court St NE
Salem OR 97301

17 Theresa Lee
18 Theresa Lee
19 Compliance Coordinator
19 Oregon Medical Board

20
21
22
23
24
25
26
27

EXHIBIT C



Steven A. LaTulippe, M.D.

531 SE Clay St., P.O. Box 787
Dallas, OR 97338
Phone: 503-623-5430
Fax: 503-831-1253

CORONAVIRUS PROTOCOL

1. Direct to ED--all patients with severe presumptive COVID symptoms: fever, chough, muscle aches, chest tightness/pain, shortness of breath.
2. Keep distance of 6 feet between all patients.
3. Minimize contact between and with patients.
4. One-way entry and exit for all patients.
5. Only one patient per room.
6. Don a mask on any patient with a cough, fever, or any suspicious viral illness.
7. Thoroughly sanitize exam room after each patient leaves room.
8. Those who refuse to come in, schedule back in 2 weeks.
9. Provide refills to next follow-up visit.
10. Patients and staff wash hands before and after each patient contact.

EXHIBIT D



**Our office is following Corona
Virus (COVID-19) protocol. We
appreciate your cooperation
and understanding during this
confusing time.**

EXHIBIT E



Steven A. LaTulippe, M.D.

531 SE Clay St., P.O. Box 787

Dallas, OR 97338

Phone: 503-623-5430

Fax: 503-831-1253

COVID-19 TREATMENT PROTOCOL

Prednisone 50-60mg 1 tab daily for 5-7 days (depending on severity of disease)

Symbicort 160/4.5 1 puff bid (until respiratory symptoms fully resolve)

Ventolin HFA 2 puffs q 1-4 hours as needed for cough/wheezing/dyspnea (better than ProAir HFA)

If at risk for secondary bacterial pneumonia:

Azithromycin 500mg 1 po daily x 3 days (pulse dose), or if more severe risk/infection,
Doxycycline 100mg 1 po bid x 10 days (also has anti-inflammatory properties)

For *any* GI symptoms, headache, myalgias (flu-like symptoms):

Pedialyte generic, 3 liters daily for 1-2 days (hold all other solids and liquids until appetite returns)

Instruct on contact precautions to reduce infectivity.

EXHIBIT F

Effectiveness of Adding a Mask Recommendation to Other Public Health Measures to Prevent SARS-CoV-2 Infection in Danish Mask Wearers

A Randomized Controlled Trial

[Henning Bundgaard, DMSc](#)

, [Johan Skov Bundgaard, BSc](#)

, ... See More

[Author, Article and Disclosure Information](#)

<https://doi.org/10.7326/M20-6817>

[Eligible for CME Point-of-Care](#)

PDF

FULL

Tools

Share

Background:

Observational evidence suggests that mask wearing mitigates transmission of severe acute respiratory syndrome coronavirus 2 (SARS-CoV-2). It is uncertain if this observed association arises through protection of uninfected wearers (protective effect), via reduced transmission from infected mask wearers (source control), or both.

Objective:

To assess whether recommending surgical mask use outside the home reduces wearers' risk for SARS-CoV-2 infection in a setting where masks were uncommon and not among recommended public health measures.

Design:

Randomized controlled trial (DANMASK-19 [Danish Study to Assess Face Masks for the Protection Against COVID-19 Infection]). (ClinicalTrials.gov: NCT04337541)

Setting:

Denmark, April and May 2020.

Participants:

Adults spending more than 3 hours per day outside the home without occupational mask use.

Intervention:

Encouragement to follow social distancing measures for coronavirus disease 2019, plus either no mask recommendation or a recommendation to wear a mask when outside the home among other persons together with a supply of 50 surgical masks and instructions for proper use.

Measurements:

The primary outcome was SARS-CoV-2 infection in the mask wearer at 1 month by antibody testing, polymerase chain reaction (PCR), or hospital diagnosis. The secondary outcome was PCR positivity for other respiratory viruses.

Results:

A total of 3030 participants were randomly assigned to the recommendation to wear masks, and 2994 were assigned to control; 4862 completed the study. Infection with SARS-CoV-2 occurred in 42 participants recommended masks (1.8%) and 53 control participants (2.1%). The between-group difference was -0.3 percentage point (95% CI, -1.2 to 0.4 percentage point; $P = 0.38$)

(odds ratio, 0.82 [CI, 0.54 to 1.23]; $P = 0.33$). Multiple imputation accounting for loss to follow-up yielded similar results. Although the difference observed was not statistically significant, the 95% CIs are compatible with a 46% reduction to a 23% increase in infection.

Limitation:

Inconclusive results, missing data, variable adherence, patient-reported findings on home tests, no blinding, and no assessment of whether masks could decrease disease transmission from mask wearers to others.

Conclusion:

The recommendation to wear surgical masks to supplement other public health measures did not reduce the SARS-CoV-2 infection rate among wearers by more than 50% in a community with modest infection rates, some degree of social distancing, and uncommon general mask use. The data were compatible with lesser degrees of self-protection.

EXHIBIT G



Zooming In: Visualizing the Relative Size of Particles

MISC

Zooming In: Visualizing the Relative Size of Particles



Published 3 months ago on October 10, 2020

By **Carmen Ang**

View the full-size version of this infographic.





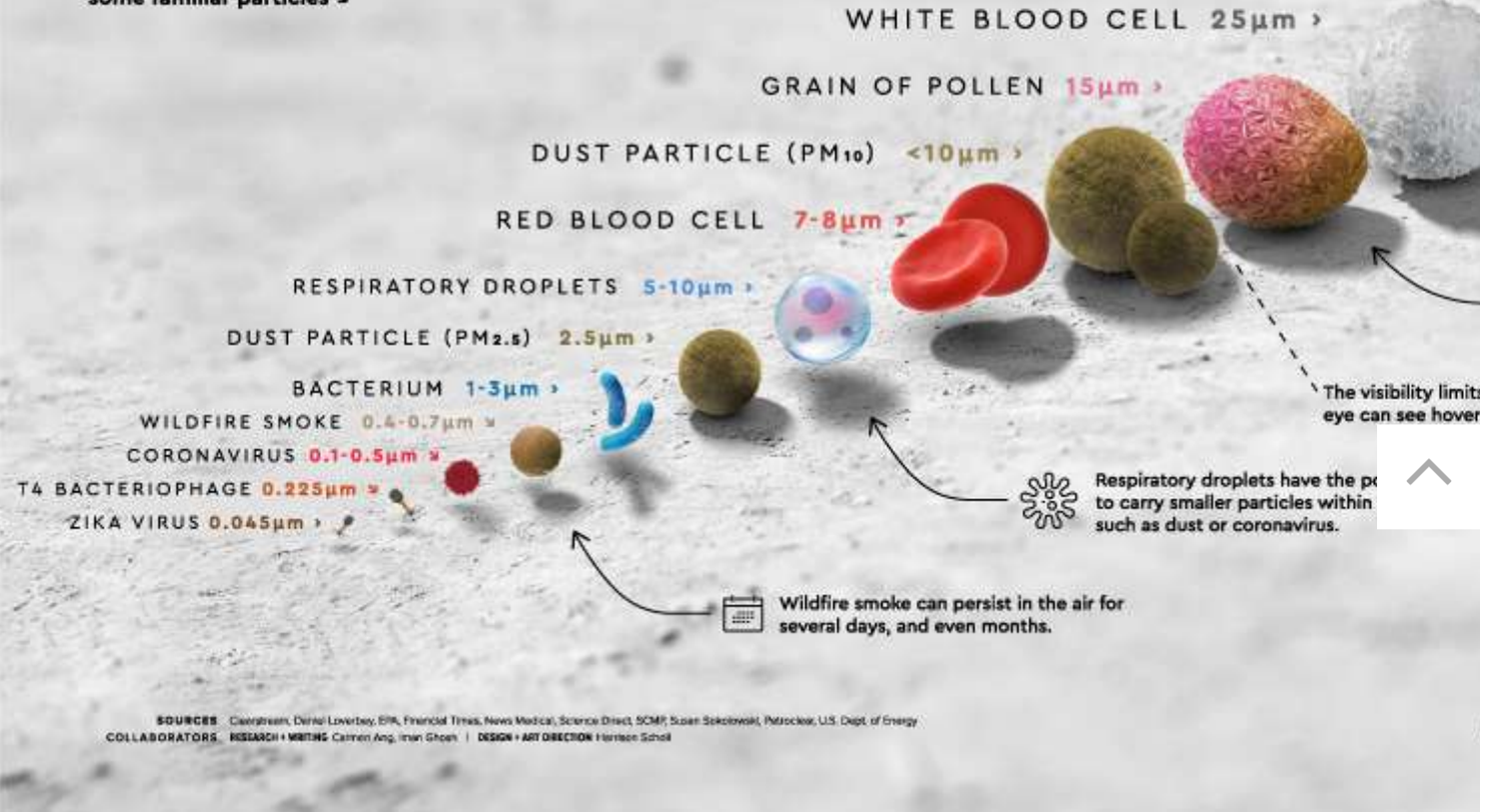
Zooming In: Visualizing the Relative Size of Particles

THE RELATIVE SIZE OF PARTICLES

From the COVID-19 pandemic to the U.S. West Coast wildfires, some of the biggest threats now are also the most microscopic.

A particle needs to be 10 microns (μm) or less before it can be inhaled into your respiratory tract. But just how small are these specks?

Here's a look at the relative sizes of some familiar particles ➤



Zooming In: Visualizing the Relative Size of Particles

View the high resolution of this infographic by [clicking here](#).

Lately, the world's biggest threats have been microscopic in size.

From the global COVID-19 pandemic to wildfires ripping through the U.S. West Coast, it's



Zooming In: Visualizing the Relative Size of Particles

Specks Too Small to See

While the coronavirus that causes COVID-19 is relatively small in size, it isn't the smallest particle out there.

Both the Zika virus and the T4 Bacteriophage—responsible for E. coli—are just a fraction of the size, although they have not nearly claimed as many lives as COVID-19 to date.

Coronavirus particles are smaller than both red or white blood cells, however, a single bacterium is still virtually invisible to the naked eye. For scale, we've also added in a single human hair as a benchmark on the upper end of the size range.

Particles	Average Size (microns, μm)
Zika virus	45nm
T4 Bacteriophage	225nm
Coronavirus	0.1-0.5 μm
COVID-19 (SARS-CoV-2)	
Bacterium	1-3 μm
Light dust particle	1 μm
Dust particle: PM2.5	$\leq 2.5\mu\text{m}$
Respiratory droplets containing COVID-19	5-10 μm
Red blood cell	7-8 μm
Dust particle: PM10	$\leq 10\mu\text{m}$
Pollen grain	15 μm
White blood cell	25 μm
Visibility threshold (Limit of what the naked eye can see)	10-40 μm
Grain of salt	60 μm
Fine beach sand	90 μm



Zooming In: Visualizing the Relative Size of Particles

particle needs to be smaller than 10 microns before it can be inhaled into your respiratory system.

Because of this, pollen or sand typically get trapped in the nose and throat before they enter the lungs. The smaller particles, however, are able to slip through more easily.

Smoky Skies: Air Pollution and Wildfires

While the virus causing COVID-19 is certainly the most topical particle right now, it's not the only speck that poses a health risk. Air pollution is one of the leading causes of death worldwide, actually deadlier than smoking, malaria, or AIDS.

One major source of air pollution is particulate matter, which can contain dust, dirt, soot, and smoke particles. Averaging around **2.5 microns**, these particles can often enter human lungs.

At just a fraction of the size between **0.4-0.7 microns**, wildfire smoke poses even more of a health hazard. Research has also linked wildfire exposures to not just respiratory issues, but also cardiovascular and neurological issues.

Here's an animated map by Flowing Data, showing how things heated up in peak wildfire season between August-September 2020:



Zooming In: Visualizing the Relative Size of Particles

HOME MARKETS TECHNOLOGY MONEY ENERGY MINING GREEN

01:36

What's the main takeaway from all this?

There are many different kinds of specks that are smaller than the eye can see, and knowing how they can impact human health. ^

Receive free **Visual Capitalist** content straight to your inbox.

Get your mind blown on a daily basis:

Your email address

Sign up for free

HOME MARKETS TECHNOLOGY MONEY ENERGY MINING GREEN



Zooming In: Visualizing the Relative Size of Particles

to Overcome

On Amazon

YOU MAY LIKE

Risk On: \$45 Billion Injected Into Stock Market Funds In One Week

The Top 50 Most Valuable Global Brands

Mapped: Drone Privacy Laws Around the World

How Every Asset Class, Currency, and S&P 500 Sector Performed in 2020

The Rich Got Richer During COVID-19. Here's How American Billionaires Performed

The Economic Impact of COVID-19 According to Business Leaders

COMMENTS

POLITICS

Visualized: The World Leaders In Positions of Power (1970-Today)

HOME

MARKETS

TECHNOLOGY

MONEY

HEALTHCARE

ENERGY

MINING

GREE



Zooming In: Visualizing the Relative Size of Particles

looks at world leaders from 1970 to today.



Published 5 hours ago on January 20, 2021

By Avery Koop



Visualized: The World Leaders In Positions of Power

Who were the world leaders when the Berlin Wall fell? How many women have been heads of state in prominent governments? And who are the newest additions to the ranks of world leaders?

This graphic reveals the leaders of the most influential global powers since 1970. Countries were selected based on the [2020 Most Powerful Countries](#) ranking from the U.S. News & World Report.

... 1 2 3 4 5 6 7 8 9 10 11 12 13 14 15 16 17 18 19 20 21 22 23 24 25 26 27 28 29 30 31 32 33 34 35 36 37 38 39 40 41 42 43 44 45 46 47 48 49 50 51 52 53 54 55 56 57 58 59 60 61 62 63 64 65 66 67 68 69 70 71 72 73 74 75 76 77 78 79 80 81 82 83 84 85 86 87 88 89 90 91 92 93 94 95 96 97 98 99 100 ...



Zooming In: Visualizing the Relative Size of Particles

POLITICS

U.S. Presidential Voting History from 1976-2020 (Animated Map)

With this map of U.S. presidential voting history by state, discover patterns that have emerged over the last twelve elections.



Published 1 day ago on January 19, 2021

By **Jenna Ross**



U.S. Presidential Voting History by State

[HOME](#) [MARKETS](#) [TECHNOLOGY](#) [MONEY](#) [HEALTHCARE](#) [ENERGY](#) [MINING](#) [GREEN](#)



Zooming In: Visualizing the Relative Size of Particles

In this graphic, we use data from the [U.S. National Archives](#) and the [MIT Election Data and Science Lab](#) to show U.S. presidential voting history by state since 1976.

Note: this post has been updated on January 19, 2021 to reflect the latest data.

[CONTINUE READING](#)

POPULAR



TECHNOLOGY / 2 months ago

50 Years of Gaming History, by Revenue Stream (1970-2020)

HEALTHCARE / 1 month ago

Tracking COVID-19 Vaccines Around the World

MARKETS / 1 month ago

The Year in Review Visualizations

MISC / 1 month ago

Chart: A Global Look at How People

MARKETS / 2 weeks ago

Prediction Consensus: What the

MISC / 3 weeks ago

Visualizing the U.S. Presidential

[HOME](#) [MARKETS](#) [TECHNOLOGY](#) [MONEY](#) [HEALTHCARE](#) [ENERGY](#) [MINING](#) [GREEN](#)



Zooming In: Visualizing the Relative Size of Particles



ABOUT MASTHEAD CAREERS ADVERTISE USE OUR VISUALIZATIONS PRESS CENTER

Copyright © 2020 Visual Capitalist

•



EXHIBIT H



AIP Physics of Fluids

[HOME](#)[BROWSE](#)[MORE ▾](#)[Home](#) > [Physics of Fluids](#) > [Volume 32, Issue 12](#) > [10.1063/5.0034580](#)

< PREV

NEXT >



Published Online: 15 December 2020

Accepted: November 2020

Effects of mask-wearing on the inhalability and deposition of airborne SARS-CoV-2 aerosols in human upper airway

Physics of Fluids 32, 123312 (2020); <https://doi.org/10.1063/5.0034580> Jinxiang Xi (奚金祥)^{1,a},  Xiuhua April Si (司秀华)², and Ramaswamy Nagarajan^{3,4}[View Affiliations](#) PDF

Topics ▾

ABSTRACT

Even though face masks are well accepted as tools useful in reducing COVID-19 transmissions, their effectiveness in reducing viral loads in the respiratory tract is unclear. Wearing a mask will significantly alter the airflow and particle dynamics near the face, which can change the inhalability of ambient particles. The objective of this study is to investigate the effects of wearing a surgical mask on inspiratory airflow and dosimetry of airborne, virus-laden aerosols on the face and in the respiratory tract. A computational model was developed that comprised a pleated surgical mask, a face model, and an image-based upper airway geometry. The viral load in the nose was particularly examined with and without a mask. Results show that when breathing without a mask, air enters the mouth and nose through specific paths. When wearing a mask, however, air enters the mouth and nose through the entire surface of the mask at lower speeds, which favors the inhalation of ambient aerosols into the nose. With a 65% filtration efficiency (FE) typical for a three-layer surgical mask, wearing a mask reduces dosimetry for all micrometer particles except those of size $1 \mu\text{m}$ – $3 \mu\text{m}$, for which equivalent dosimetry with and without a mask in the upper airway was predicted. Wearing a mask reduces particle penetration into the lungs, regardless of the FE of the mask. The results also show that mask-wearing protects the upper airway (particularly the nose and larynx) best from particles larger than $10 \mu\text{m}$ while protecting the lungs best from particles smaller than $10 \mu\text{m}$.



I. INTRODUCTION

Infectious respiratory diseases spread when a healthy person comes in contact with virus-laden droplets from someone who has been infected, often through a sneeze or cough.^{1,2} Wearing a mask has been proven to be an effective method of protection in this pandemic, which both reduces the exhalation of virus-laden aerosols from a COVID patient and minimizes the inhalation of airborne virus-laden aerosols by the subjects surrounding the patient.^{3,4} Masks are available with different filtration efficiencies and levels of breathability. The filtration media are often made of micrometer or nano-sized fibers, arranged as a matrix or network, to achieve the desired filtration efficiency (FE).⁵ A mask with a higher FE often has a higher breathing resistance, i.e., worse breathability.

Physiological studies show that the SARS-CoV-2 virus that causes COVID-19 first deposits in the human upper airway to cause infection of the nasal goblet secretory cells and then spreads to the central and inner parts of the lungs.^{6,7} The final target is the alveoli, the smallest respiration units that has a diameter of 0.2 mm–0.4 mm.^{8,9} The virus will attack the type-II cells in the alveoli and interfere with their capacity to secrete the surfactants needed to maintain normal breathing.⁶ With an inadequate lining of surfactants on the alveolar wall, water surface tension can increase the breathing effort by two to four times to draw in the same volume of fresh air (or oxygen).¹⁰ To make things worse, the coincidence of hypertension of the cardiovascular system can fill the alveolar airspace with fluids, making breathing and oxygen exchange even harder.¹¹ Usually under this condition, mechanical ventilation to the patients is needed.



dose in both concentration and time) that are necessary to cause the illness.^{12,13} It is currently unclear what the exact infectious dose is for COVID-19, but it is estimated to be 1000 viruses, by analogy to influenza and SARS.^{14–17} Therefore, the knowledge of the local deposition rates of the virus-laden particles on the epithelial cells (i.e., viral loads) is crucial in determining the risk of COVID infection. Due to face covering, both inhaled and exhaled airflow can be altered significantly. Simha and Rao visualized the expiratory flows of coughs and quantified the propagation distances with and without a mask using a Schlieren imaging system. It was demonstrated that the cough flow fields were governed by the propagation of viscous vortex rings. Verma *et al.*^{19,20} used a laser-illuminating system to visualize the effectiveness of face masks and face shields in obstructing respiratory jets. Their results confirmed that a well-fitted mask can significantly curtail the speed and range of expelled droplets while a face shield still allowed droplets to move around and spread out over a large area.^{19,20} However, how the presence of a mask affects the inhalation dosimetry of ambient aerosols in the upper airway is not clear, even though we expect certain degrees of difference from that without wearing a mask. In contrast to the recent resurgence of interest in using Schlieren and (particle image velocimetry) systems to visualize expiratory flows,^{18–22} reports of inspiratory flow and particle dynamics with face-covering are scarce, with the exception of a very recent study by Dbouk and Drikakis,²³ who elegantly simulated the effectiveness of face-covering on reducing airborne viral infections. This lack of investigation into inhalation dosimetry with masks can be largely attributed to the inaccessibility of measurement within the mask and in the human respiration tract.



wearing a mask, it is hypothesized that the inhalability of airborne particles into the nose/mouth, as well as their subsequent deposition within the upper respiratory tract and lungs, can also be significantly different.

The objective of this study is to numerically characterize the difference in the deposition distribution of ambient aerosols in the upper airway with and without a mask. The specific aims include:

- (1) developing a computational model that includes a mask, face, and upper airway with a perfect mask–face seal,
- (2) studying the inspiratory airflows and particle motions near the face when wearing a surgical mask in comparison to those without a mask,
- (3) characterizing the effect of particle size, inhalation flow rate, and mask resistance matrix on the dosimetry of ambient aerosols with and without a mask, and
- (4) quantifying the fraction of airborne particles deposited on the face, retained in the upper airway, and entering the lungs; regional deposition in the nose and larynx will be particularly examined.

The results of this study will provide insights into the airflows and particle dynamics with a mask on and the factors involved in determining the protection efficacy of face-covering, which is an area remaining largely unexplored but will be of high interest to patients, care providers, PPE designers, and public policymakers.

II. METHODS



A. Mask-face-airway model

The computational model consisted of three parts: a realistic model of a disposable three-layer surgical mask, a face model with spherical ambient airspace, and an upper airway model with the nose, mouth, pharynx, and larynx [Fig. 1(a)]. The upper airway model was connected to the face seamlessly by fusing the nostrils and mouth opening to the corresponding regions of the face [Fig. 1(b)]. The mask model was then appended to the face by covering the mouth and nose and was fit tightly to the face. The mask–face interface is shown in Fig. 1(b) as a close-loop strip (light blue), within which the face will be covered by the mask [yellow color, Fig. 1(b)], and the rest of the face is exposed to the environment.

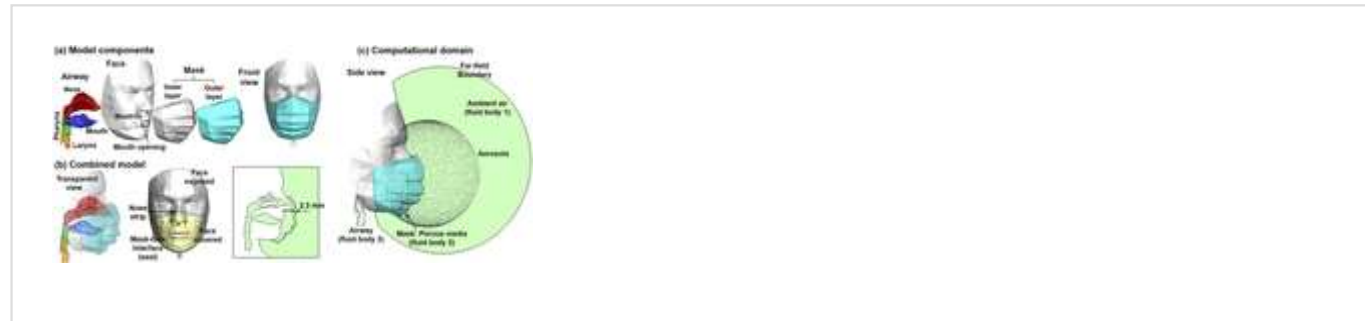


FIG. 1. Mask-face-airway model: (a) model components: upper airway (nose, mouth, pharynx, and larynx), face with nostrils and mouth opening, and mask with inner and out layers; (b) the combined model with the upper airway being connected to the face and the mask fitted on the face with no leakage; and (c) the computational domain with spherical ambient airspace and a spherical aerosol profile. There are three fluid bodies: ambient air (fluid body 1), mask

in (b)], delineated by the mask–face interface (seal) and the nasal strip.

[!\[\]\(c27be48f17fe8ecbb38b20ac0bca5a5b_img.jpg\) PPT | High-resolution](#)

Individually, the upper airway geometry was a combination of a nasal cavity, an oral cavity, and a pharyngolaryngeal region, which were developed separately in our previous studies. In brief, the nose model was reconstructed from MRI scans of a 53-year-old subject with no rhinology disorders.^{24,25} The oral cavity was modified from the mouth model developed by Xi and Longest,²⁶ which was further based on an oral cast reconstructed from a dental impression by Cheng *et al.*²⁷ The surgical mask model was specifically developed for this study using open-source 3D rendering software Blender (Blender Foundation, Amsterdam, the Netherlands) based on photos of a subject wearing a disposable three-layer surgical mask from different angles. Morphological details, such as the three folds (or pleats) on the mask, were retained. To avoid the compounding effect of mask–face sealing effects, a perfect mask–face fit was assumed in this study. In doing so, the mask model as a volume was extended backward to intersect with the human face. By deleting the parts of the mask that fall behind the face, a seamless mask–face seal was achieved [Fig. 1(b)].

B. Flow-particle modeling

[!\[\]\(c304765eaff2580582d718e36e0c4ff0_img.jpg\) PDF](#)

and airway (fluid body 3), as shown in Fig. 1(C). Porous media were adopted to simulate the resistance of the mask, whose properties are described in detail in Sec. II C. Airflow was assumed to be incompressible ($\rho = 1.204 \text{ kg/m}^3$) and isothermal (20°C) with a dynamic viscosity of $1.825 \times 10^{-5} \text{ kg/m s}$. To simulate inspiratory airflows, zero gauge pressure was specified at the far-field boundary, and a negative flow rate was specified at the trachea opening [Fig. 1(c)]. The airflow was drawn in by the negative pressures in the airway from the ambient airspace, through the mask, and into the oronasal openings, with a pressure drop across the mask and modified airflows around the mask. Considering the multiple flow regimes that may exist in the ambient airspace and respiratory tract, the low Reynolds number (LRN) $k-\omega$ turbulence model was used to simulate the inspiratory airflows based on its ability to accurately predict pressure, velocity, and shear for transitional and turbulent flows.²⁸ Moreover, it has been demonstrated to provide an accurate solution for laminar flow as the turbulent viscosity approaches zero.²⁹ For more details of the LRN $k-\omega$ turbulence model, refer to the work of Wilcox.²⁹

To simulate the inhalation dosimetry of airborne aerosols, a spherical profile of monodisperse particles was generated that surrounded the face with an approximate distance of 0.10 m. The particle motions were tracked using a discrete phase Lagrangian tracking algorithm enhanced with user-defined functions (UDFs) for the near-wall treatment of flow and particle velocities.^{30,31} Physical properties of the particles include a spherical shape and a particle density ρ_p of 1.0 g/cm^3 . The transport equations are expressed below:

$$dv_i = Du_i - f - \frac{dx_i}{dt}$$



Here, v_i and u_i are particle and flow velocities, respectively, α is the flow-particle density ratio, f is the drag factor, and $\tau_p = \rho_p d_p^2 / 18\mu$ is the particle relaxation time (i.e., the time for a particle to respond to local flow changes). One-way coupling (from flow to the particle) was assumed for ambient aerosols ranging from $1\text{ }\mu\text{m}$ to $20\text{ }\mu\text{m}$ with main flow tracking. This UDF-enhanced Lagrangian particle-tracking model had shown high fidelity in matching *in vitro* dosimetry of both nanometer^{32,33} and micrometer particles.^{34,35}

C. Mask material properties

A mask is characterized by its filtration efficiency (FE) and permeability (or breathability). It is noted that even though a high-filtration mask often has a high flow resistance, these two parameters can be independent of each other. A surgical mask with an experimentally measured FE (65%) and porosity (10%) was used in this study,³⁶ where the FE was measured using TSI 8130 (TSI Incorporated) and the porosity was quantified using SEM images of the mask sample. A mask FE of 0%, where all particles passed through the mask with no deposition, was also considered to represent the worst scenario of wearing a mask. Considering a 0% FE mask also allows the study of the impact of the mask-altered flow field alone on particle inhalability. It is noted that particle deposition in the mask cannot be directly simulated in ANSYS Fluent (Canonsburg, PA); rather, all particles that come into contact with the mask will pass through it. Post-processing was needed to calculate the deposition fraction (DF) on the face separately,

on the uncovered face [gray, Fig. 1(b)] and 35% of the particles depositing on the mask-covered face [yellow, Fig. 1(b)]. For the DFs in the upper airway and lungs, only 35% of the deposited particles were counted since 65% were filtered out by the mask.

The viscous resistance of the mask in the normal direction was calculated from Darcy's law using the flow rate (85 l/min) and pressure (~ 96 Pa) measured by TSI 8130^{36,37} as follows:

$$\text{Viscous Resistance} = \frac{\Delta P}{(Q/A) \mu L}. \quad (2)$$

The viscous resistance was calculated as a bulk value of 8.864×10^9 1/m² based on a sampling area $A = 55$ cm², a dynamic viscosity $\mu = 1.825 \times 10^{-5}$ kg/m s, and an overall mask thickness $L = 2.3$ mm without differentiating the three layers that comprise the surgical mask [Fig. 1(b)]. It is noted that the resistance of the mask can be different in lateral directions. To investigate the resistance matrix effects on airflow and particle dynamics near the face and inside the airways, five resistance matrices were considered, with the lateral viscous resistance many times that in the normal direction. These include 1-1-1, 3-1-3, 6-1-6, 10-1-10, and 10-10-10, with "1" representing the normal resistance (8.864×10^9 1/m²), "3" representing three times that of the normal resistance (2.659×10^{10} 1/m²), and so on. The mask resistance matrix 1-3-1 was used as the control case and was examined for all particle sizes (1 μm -20 μm) and four flow rates (15 l/min, 30 l/min, 45 l/min, and 60 l/min); however, for the other four resistance matrices, only 30 l/min was considered. For all simulations with a mask, a case without a mask was simulated to understand the effects of

D. Numerical methods

ANSYS Fluent (Canonsburg, PA) was used to simulate inspiratory airflows and particle motions. User-defined functions were implemented to specify the airborne aerosol distribution, calculate the deposition fractions (DFs), and plot the spatial distribution of deposited particles.³⁸ The deposition enhancement factor (DEF), which represents the ratio of local DF over the average DF, was used to visualize the intensity of deposition at a cellular level.³⁹ Considering the large size differences among the ambient airspace, mask, and airway, a multi-scale, multi-domain mesh was generated using ANSYS ICEM CFD (Ansys, Inc.) [Fig. 2(a)]. To capture the near-wall velocity variation, a four-layer body-fitted prismatic mesh was specified near the face and in the airway, with a height of 0.03 mm in the first layer [Fig. 2(b)]. A grid-independent study was conducted using six mesh densities, i.e., 1.13×10^6 , 1.87×10^6 , 2.98×10^6 , 3.97×10^6 , 4.93×10^6 , and 6.24×10^6 . The grid-independent results were achieved at 4.93×10^6 , where the variation in the nasal deposition fraction was less than 1% relative to that at 6.24×10^6 . Considering that quantifying the particle deposition fraction is inherently a statistical process, a sufficient number of sample particles are needed to attain statistically converged (i.e., particle-count independent) deposition results. In doing so, the number of released particles was increased from 10 000 to 100 000, with an increment of 5000 particles. The particle-count independent results were achieved at 60 000 particles when the variation in the nasal deposition was less than 0.5% between two consecutive tests.



FIG. 2. Computational mesh: (a) multi-scale, multi-domain mesh, with coarse mesh in the ambient airspace, fine mesh on the face and mask, and ultrafine mesh in the airway and (b) body-fitted mesh was used in the near-wall region of the airway, with four layers of prismatic cells and a height of 0.03 mm in the first layer, as displayed in the oropharyngeal carina and the glottis.

[PPT | High-resolution](#)

III. RESULTS

A. Airflow and particle dynamics with and without a mask

1. Airflow

Wearing a mask can notably distort the inhalation aerodynamics in comparison to that without a mask. Figure 3 shows the comparison between inspiratory airflow and pressure fields at 30 l/min with and without a mask in terms of pressure distributions, velocity contours, streamlines, and vector fields near the oronasal openings. As expected, wearing a mask caused an abrupt pressure drop of 22 Pa across the mask, which had a resistance matrix of $3a-a-3a$, where $a = 8.864 \times 10^9 \text{ l/m}^2$. As a result the total pressure drop between the ambient and trachea was about

[PDF](#)

addition, flow streamlines across the mask were notably refracted (i.e., turning aside from their straight paths with various angles), especially in the vicinity of the mask pleats (or folds), as shown in the second panel of Fig. 3(a). By comparison, all streamlines entering the airway without a mask are smooth. These flow distortions from a mask were further illustrated by the velocity contour in the mid-plane [third panel of Fig. 3(a)]. With a range of 0.0 m/s–0.2 m/s, the airflow speeds are noticeably higher near the mask pleats than other regions (i.e., smooth surface) of the mask, which are clearly different from the smooth velocity contours without a mask. The fourth panel compares the vector fields at the mid-plane with and without a mask. One apparent difference was the higher flow speed near the mask pleats, indicating a significant impact from the physical properties of the mask (i.e., shape, size, resistance, orientation, etc.). As these mask folds are located below the mouth and nose, the flow entering the nose after a mask appears more aligned with the nostril orientation than that without a mask (fourth panel, Fig. 3).



FIG. 3. Comparison of inspiratory airflows at 30 l/min between two scenarios, (a) with a mask and (b) without a mask in terms of the mid-plane pressure contour (first panel), velocity contours and

vector field (fourth panel), and velocity of fluid particles passing the mask (fifth panel). Wearing a mask significantly distorted the airflow and pressure distributions.

[!\[\]\(8f8f1f5b19afd555c2b0207a25ba97d3_img.jpg\) PPT | High-resolution](#)

The rightmost panels of Fig. 3(a) visualize the velocities of airflow through a mask with massless particles at an inhalation flow rate of 30 l/min. To simulate the scenario without a mask, the porous media resistances were specified as zero [rightmost, Fig. 3(b)]. With no obstructions from the mask, patches of high-speed airflows (i.e., convection zones) are observed that are apparently related to nasal and oral ventilations. With a mask, however, the flow is more widespread on the mask, with elevated speeds near the mask folds [rightmost, Figs. 3(a) vs 3(b)]. Due to the mask resistance, inspiratory airflows are slowed down in the otherwise convective respiration zones. At the same time, as the same amount of air will be inhaled, they approach the oronasal openings through other regions of the mask. With an overall lower speed of carrier airflows, the inhalability of entrained particles can be altered, especially into the nostrils, which orientate downward 30°–45° relative to the gravitational orientation.

Wearing a mask had an insignificant effect on the oronasal flow partition, which was found to be 61:39 (i.e., mouth:nose) with a mask and 60:40 without a mask. The flow Reynolds number ($Re = \rho UL/\mu$, with U being the local velocity and $L = 9$ mm being the characteristic length at the outlet) was estimated to be 327 in the nose, 520 in the mouth, 965 in the pharynx,

2. Particle dynamics

Particle dynamics at an inhalation flow rate of 30 l/min with and without wearing a mask are shown in Fig. 4. First, particles move slower when wearing a mask due to the mask resistance. As a result, particles advance a shorter distance than without wearing a mask during the same period of time [Figs. 4(a) vs 4(b)]. Second, particle behaviors are highly sensitive to the particle size. While 1- μm particles closely follow the inspiratory airflows, large particles of 10 μm and 20 μm exhibit drastically different patterns due to the escalating gravitational effect. As the inhalability of micrometer particles is a tag-war result between the convection and gravitational sedimentation, the presence of a mask, as well as the altered particle motions that are incurred, can perceptibly change the particle inhalability, as well as the dosimetry distribution in the downstream airways.

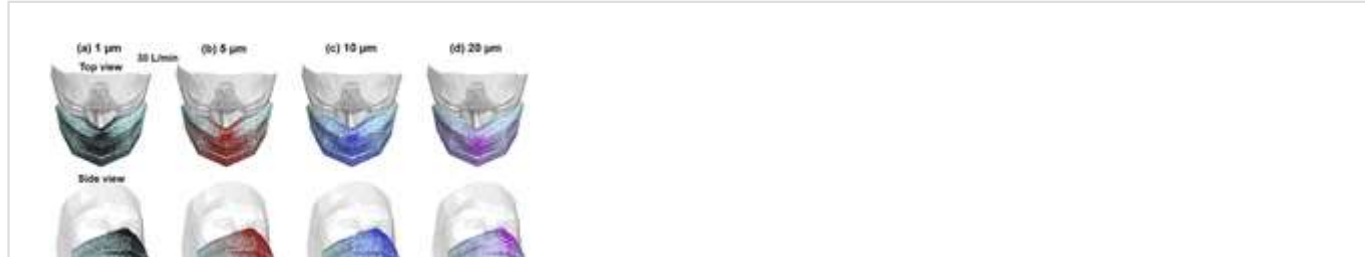


FIG. 4. Instantaneous snapshots of particle positions in MO at different times after their release during (a) the first cycle and (b) the second cycle.

B. Particle deposition with and without a mask

1. Deposition on the mask

Figure 5 shows the particle deposition on the mask at 30 l/min for various particle sizes. Overall, similar deposition patterns are noted among the particle sizes considered ($1\text{ }\mu\text{m}$, $5\text{ }\mu\text{m}$, $10\text{ }\mu\text{m}$, and $20\text{ }\mu\text{m}$), with subtle variations becoming progressively noticeable with increasing particle size. For instance, few $20\text{-}\mu\text{m}$ particles come in contact with the mask than smaller particles. This decrease is most obvious in the lower folds [hollow arrows, Figs. 5(c) and 5(d)] of the mask. Considering that particle overlapping may prevent an accurate assessment of the dosimetry, the deposition enhancement factor (DEF) was plotted to visualize the deposition intensity as the ratio of the local deposition rate to the average deposition rate. A range of 0–10 was adopted to identify the zones with deposition one order of magnitude higher than the mean dosimetry. As shown in the lower panels of Figs. 5(a)–5(d), elevated deposition occurs along the vertical middle line of the mask, as well as within the mask folding. As the particle size increases, the deposition hot zones decrease in the middle of the mask. For $20\text{-}\mu\text{m}$ particles, elevated dosimetry that is one order of magnitude higher than the mean can only be found at the top of the mask [arrow, lower panel, Fig. 5(d)].



[PDF](#)

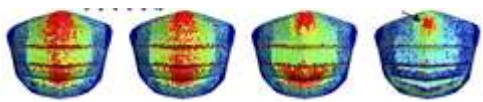


FIG. 5. Particle deposition pattern and intensity on the mask at 30 l/min for particles of (a) $1\text{ }\mu\text{m}$, (b) $5\text{ }\mu\text{m}$, (c) $10\text{ }\mu\text{m}$, and (d) $20\text{ }\mu\text{m}$, with a top view, a side view, and a visualization of particle localizations in terms of the DEF (deposition enhancement factor).

[PPT | High-resolution](#)

2. Face, upper airway, and lungs

A comparison of particle deposition on the face with and without a mask is shown in Fig. 6 for different particle sizes. Smaller particles give rise to more dispersed deposition on the face, regardless of wearing a mask or not. For $1\text{-}\mu\text{m}$ particles, deposition is spotted around the eyes, which are venerable sites of bacterial or viral infections. Interestingly, wearing a mask leads to a higher deposition underneath the eyes [top panel, Fig. 6(a)] than without a mask. As the particle size increases from $1\text{ }\mu\text{m}$ to $20\text{ }\mu\text{m}$, more particles deposit on the nose and the forehead. In comparison to the deposition with a mask, one major difference is the enhanced deposition in the philtrum, the region below the nose and above the upper lip (second row). The deposition intensities were also compared with and without a mask in terms of the DEF in the third and fourth rows, as shown in Figs. 6(a)-6(d), respectively. Again, the dispersed deposition for $1\text{-}\mu\text{m}$ particles, the increasingly concentrated deposition on the nose and forehead with particle size, and the higher deposition on the philtrum are more vividly

[PDF](#)

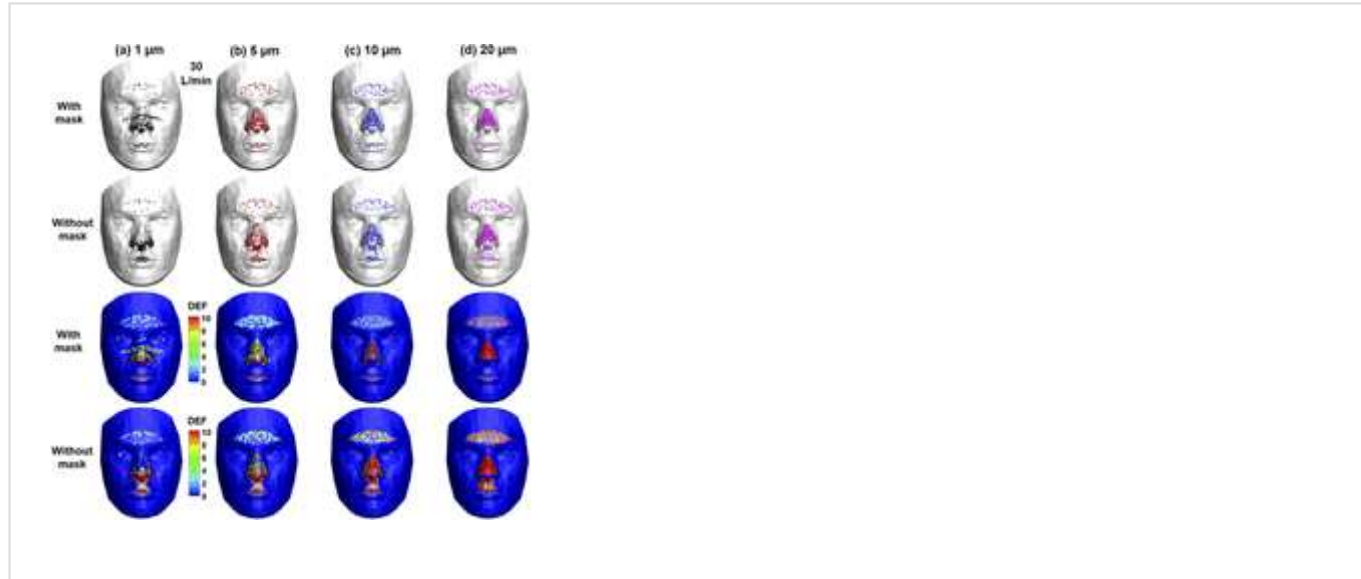


FIG. 6. Comparison of the particle deposition pattern and intensity on the face (a) with a mask and without a mask at an inhalation flow rate of 30 l/min for particles of 1 μm , 5 μm , 10 μm , and 20 μm . The deposition intensities were visualized using the DEF (deposition enhancement factor).

[↓ PPT | High-resolution](#)

Figure 7 compares the dosimetry of ambient aerosols at 30 l/min with and without a mask in terms of face deposition, airway deposition, and penetration rate into the lungs. It is noted that the deposition fraction (DF) with a mask was presented in two formats: (1) “before correction” that assumed zero mask filtration (red hollow delta) and (2) “after correction” that assumed 65% mask filtration (red filled delta). Regarding the face deposition with a mask, the DF after correction was calculated by including 35% of the particles that came in touch with the mask’s outer layer and

[↓ PDF](#)

Much to our surprise, by assuming zero filtration efficiency, wearing a mask leads to significantly higher deposition on the face for all particles considered ($1 \mu\text{m}$ – $20 \mu\text{m}$) and in the airway for particles of $1 \mu\text{m}$ – $10 \mu\text{m}$ [Fig. 7(a)]. With a 65% filtration efficiency, which is typical for a three-layer surgical mask, the corrected face deposition falls below the unmasked DFs for all particles, despite a close match for $15\text{-}\mu\text{m}$ particles.

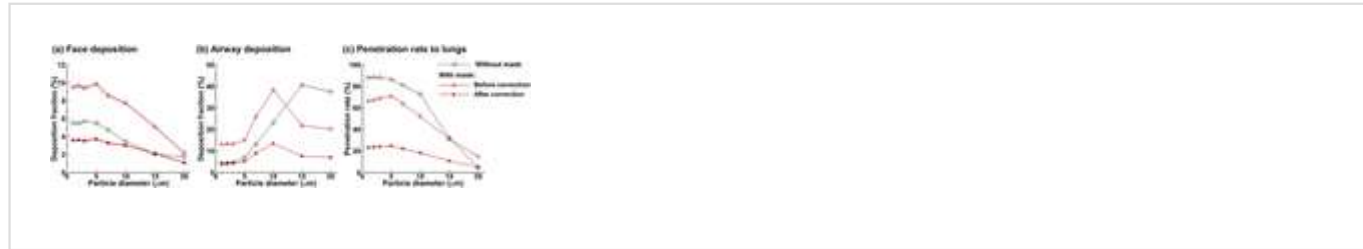


FIG. 7. Comparison of the fate of inhaled aerosols at 30 l/min with (red lines) and without (black line) wearing a mask in terms of (a) face deposition, (b) airway deposition, and (c) penetration rate into the lungs. When wearing a mask, two scenarios were considered, with the filtration efficiency being 0% in the first scenario (i.e., before correction, hollow delta, representing the worst limit) and 65% in the second scenario (i.e., after correction, solid delta, representative of a typical three-layer surgical mask). A pass rate of 35% was applied for all particles that came in contact with the outer layer of the mask. For instance, the number of particles depositing on the face was counted as that of particles landing on the uncovered face plus the 35% of particles landing on the face covered by the mask.

[PPT | High-resolution](#)

[PDF](#)

hollow delta) led to a higher deposition of $1\text{ }\mu\text{m}$ - $10\text{ }\mu\text{m}$ particles but a lower deposition of $15\text{ }\mu\text{m}$ - $20\text{ }\mu\text{m}$ particles than without a mask (blue dotted circle). The corrected airway DF (red filled delta) fell below the unmasked one (blue dotted circle) for particles larger than $3\text{ }\mu\text{m}$ but is still comparable for small particles of size $1\text{ }\mu\text{m}$ - $3\text{ }\mu\text{m}$. Figure 7(c) quantifies the penetration rate of particles into the lungs. In this case, wearing a mask indeed reduces the chance of ambient particles getting into the lungs for all particles considered except for $20\text{ }\mu\text{m}$ ones, which fortunately have very low inhalability due to their weight.

3. Regional deposition in the nose, mouth, pharynx, and larynx

Considering that epitheliums in different sections of the respiratory tract have varying susceptibility to inhaled agents, the dosimetry in the upper airway [Fig. 7(b)] was further separated into four regions, nose, mouth, pharynx, and larynx, as shown in Fig. 8(a) (before correction) and Fig. 8(b) (after correction). It is clear that wearing a mask not only changes the overall DF in the upper airway but also the DF distribution among the four regions. Figure 8(c) shows the comparison of the nose deposition with (after correction) and without a mask. In contrast to the high sensitivity of the nasal DF to particle size without a mask, the nasal DF was found to be relatively independent of the particle size when wearing a mask. On the other hand, the laryngeal DF shows high sensitivities, regardless of the presence of a mask. These particle-size-dependent differences highlight the need for future testing of mask filtration efficiency of monodisperse aerosols. Future estimation of infectious respiratory disease transmission and presentation should also consider these size-related discrepancies for more reliable predictions. The surface deposition in the upper airway is

with and without a mask. Heterogeneous particle distributions are found in all cases hereof, with high levels of particle accumulations in certain areas while no or few particles in other areas. Note the highly different deposition patterns among the four different sized aerosols with a mask shown in the upper panel of Fig. 8(e). Even though the cumulative deposition in the nose may be insensitive to particle size, the local deposition can still be highly sensitive, corroborating the need to study monodisperse aerosols.



FIG. 8. Regional deposition fractions (DFs) at 30 l/min in different sections of the upper airway (i.e., the nose, mouth, pharynx, and larynx): (a) DFs without a mask vs DFs with a mask before correction (with 0% mask filtration efficiency), (b) DFs without a mask vs DFs with a mask after correction (with 65% mask filtration efficiency), (c) the nose DF without a mask vs with a mask after correction, (d) the larynx DF without a mask vs with a mask after correction, and (e) surface deposition in the upper airway for particles of sizes 1 μm , 5 μm , 10 μm , and 20 μm .

[!\[\]\(785d8b53f116faca2dbae2cbde4b497e_img.jpg\) PPT](#) | [High-resolution](#)

C. Effect of the inhalation flow rate and mask resistance

1. Inhalation rate effects

In the above-mentioned sections, we have examined in detail the dosimetry of ambient aerosols with and without a mask for one flow rate (30 l/min) and one mask (with a resistance matrix of 3-1-3). The impacts from different flow rates and mask resistance matrices were also investigated as presented in Figs. 9 and 10, respectively. Figure 9(a) provides further support that the presence of a zero-filtration mask could lead to higher deposition on the face for micrometer particles. Moreover, this deposition enhancement increases with the increasing inhalation flow rates [upper panel, Fig. 9(a)]. As shown in Fig. 8(a), after considering the 65% mask filtration efficiency, the corrected face dosimetry with a mask falls below that without a mask for all particles, except 15 μm and 20 μm particles [lower panel, Fig. 9(a)]. Similar trends are also observed in Fig. 9(b) for airway deposition, where the uncorrected DFs with a mask are higher than those without a mask for particles smaller than 10 μm and lower for particles of size 15 μm -20 μm . As the inhalation flow rate increases, the deposition in the airway quickly increases for both scenarios, with and without a mask. This increase is especially pronounced for large particles (10 μm -20 μm), whose inhalability is strongly affected by gravity and is increased by intensifying convective effects. Considering Fig. 9(c), increasing the flow rates decreases the penetration rate into the lungs

[!\[\]\(eb5d9e0737fbe725ec1d928d9e93588b_img.jpg\) PDF](#)

associated particle depletion. For all flow rates considered, wearing a mask reduces the lung dosimetry (trachea and below), regardless of the mask filtration efficiency. Wearing a 65%-filtration mask reduces the lung deposition by 2.5–3.5 folds for particles of size $1 \mu\text{m}$ – $10 \mu\text{m}$ [lower panel, Fig. 9(c)].

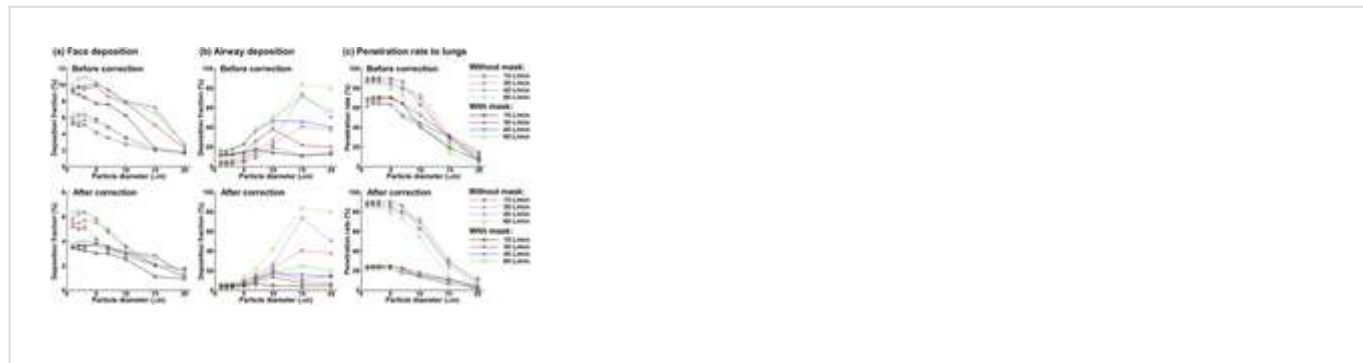
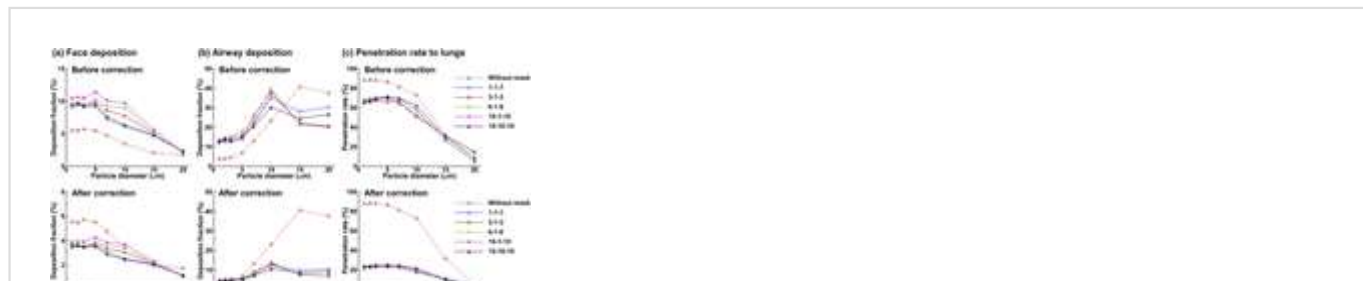


FIG. 9. Effects of the flow rate on the fate of inhaled aerosols with (solid lines) and without (dashed lines) wearing a mask in terms of (a) face deposition, (b) airway deposition, and (c) penetration rate into the lungs. The upper panels show the scenario with 0% mask filtration (i.e., before correction), and the lower panel shows the modified rates with a mask filtration efficiency of 65% (i.e., after correction).

[↓ PPT | High-resolution](#)



[↓ PDF](#)

FIG. 10. Effects of the mask resistance matrix on the fate of inhaled aerosols at 30 l in comparison to the scenario without a mask: (a) face deposition, (b) airway deposition, and (c) penetration rate into the lungs. The upper panels show the scenario with 0% mask filtration (i.e., before correction), and the lower panel shows that with 65% mask filtration (i.e., after correction).

[!\[\]\(ee63952771dcddb5555d089c684847fd_img.jpg\) PPT | High-resolution](#)

2. Mask resistance matrix effects

The effects of the mask resistance matrix on particle dosimetry with and without a mask are shown in Fig. 10 at an inhalation flow rate of 30 l/min. Masks with four additional resistance matrices were considered, i.e., 1-1-1 (homogeneous), 6-1-6, 10-1-10, and 10-10-10 (homogeneous with ten times resistance). Note that 1-1-1 represents a resistance matrix of 8.864×10^9 1/m² in all three directions, while 10-1-10 represents 8.864×10^{10} in lateral directions and 8.864×10^9 in the normal direction. Increasing the lateral resistances (x and z directions) consistently increases the face deposition, with the highest face DF predicted for the 10-1-10 matrix [Fig. 10(a)]. Similar face DFs were predicted between the two homogeneous masks with a resistance difference of one order magnitude (i.e., 1-1-1 and 10-10-10), as shown in Fig. 10(a). However, consistent lower deposition in the upper airway was predicted with the 10-10-10 matrix than the 1-1-1 matrix [upper panel, Fig. 10(b)] presumably because of the lower particle speeds and the associated lower inhalability of ambient particles after the mask of higher

[!\[\]\(f063ef9e16f4c52ea7f0906a8473add2_img.jpg\) PDF](#)

upper airway was predicted by wearing a mask with 65% filtration efficiency for all particles larger than $5 \mu\text{m}$ [lower panel, Fig. 10(b)].

Insignificant influences from the variation of the resistance matrix were found on the particle penetration rate into the lungs for all micrometer particles considered [Fig. 10(c)].

3. Variation of face deposition

Figure 11 shows the deposition variation on the mask under the influences of different flow rates and mask resistances. For $10-\mu\text{m}$ particles [Fig. 11(a)], the deposition hot zones were spotted at the top and bottom of the mask for an inhalation rate of 15 l/min . These two deposition hot zones constantly grew in size with an increasing flow rate from 15 l/min to 60 l/min [Fig. 11(a)]. Deposition in the mask pleats also intensified with increasing flow rates. For $20-\mu\text{m}$ particles [Fig. 11(a)], similar trends were observed in the deposition hot zones with consistently smaller areas at the corresponding flow rates. Due to a larger gravity effect, a V-shaped deposition hot zone formed in the lower ridge of the third mask folding at 45 l/min and 60 l/min [hollow arrows, Fig. 11(b)]. The effects of mask resistance homogeneity (or deviation from it) on the mask deposition (or the respirable particles passing through the mask) are demonstrated in Fig. 11(c). Compared to the relatively even distribution of particle depositions in the two homogeneous masks (1-1-1 and 10-10-10), intensified deposition occurred along the vertical middle line in the two masks with heterogeneous resistances [Fig. 11(c)].



PDF



FIG. 11. Deposition variation on the mask under different inhalation flow rates for (a) 10- μm particles, (b) 20- μm particles, and (c) with different mask resistances (i.e., filter matrix in three directions: 1-1-1, 6-1-6, 10-1-10, and 10-10-10) for 5- μm particles at 30 l/min.

[PPT | High-resolution](#)

4. Variation of deposition in the nose, mouth, pharynx, and larynx

The effects of the inhalation flow rate on regional DFs in the upper airway are presented in Figs. 12(a)-12(c) for 15 l/min, 45 l/min, and 60 l/min, respectively. Including the case of 30 l/min shown in Fig. 8, it is observed that both the total and regional DFs in the upper airway are sensitive to the inhalation flow rates, which affect the particle inhalability into the airway, as well as the particle transport within the airway, by determining the convective effects vs gravitational sedimentation. Even though the presence of an all-pass mask (i.e., zero filtration efficiency) increases the airway deposition for all flow rates considered, this increase is more significant at lower flow rates for small micrometer particles (right panels, Fig. 12). As a result, noticeably higher DFs were predicted for 1 μm -3 μm particles at 15 l/min by wearing a mask of 65% filtration efficiency than without a mask [the insert panel in Fig. 12(a)]. Even though this abnormality

[PDF](#)

in magnitude at 60 l/min with a 65%-filtration mask vs no mask [the insert panel in Fig. 12(c)].

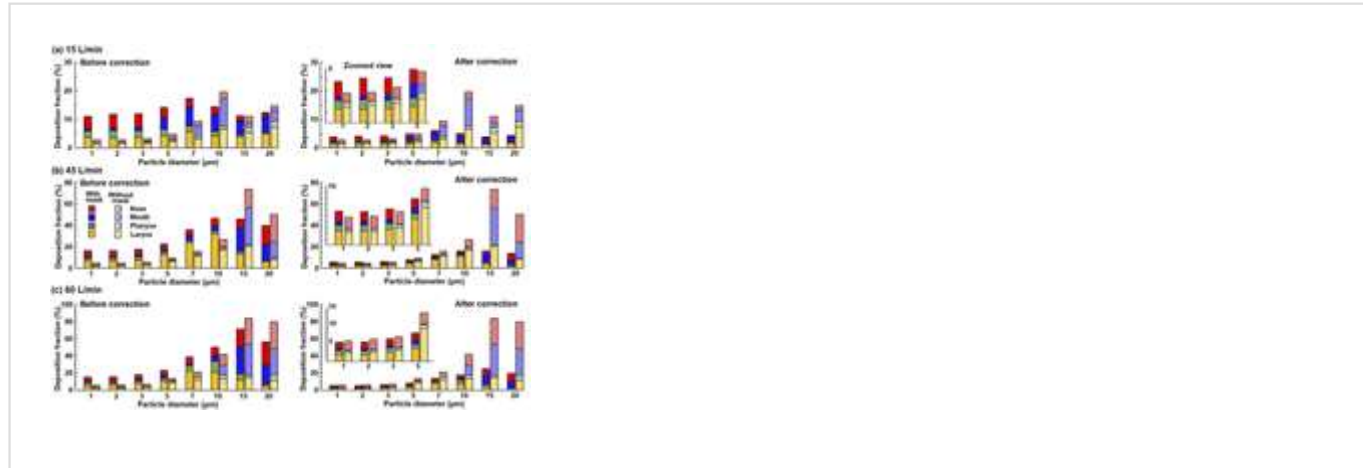


FIG. 12. Deposition distribution in different sections of the upper airway (the nose, mouth, pharynx, and larynx) under varying breathing conditions: (a) 15 l/min, (b) 45 l/min, and (c) 60 l/min. The left panels compare the DFs without a mask vs DFs with a mask before correction (with 0% mask filtration efficiency), while the right panels compare the DFs without a mask vs DFs with a mask after correction (with 65% mask filtration efficiency). Zoomed inserts for particles of 1 μm -5 μm are shown in the three right panels.

[↓ PPT | High-resolution](#)

The dosimetry of ambient aerosols in the nose or larynx can be very different between scenarios with and without a mask at different flow rates. At 15 l/min, the particle deposition in the nose with a 65%-filtration mask peaked at 2 μm and decreased with increasing particle size, whereas the deposition with no mask peaked at 10 μm [top panel Fig. 13(a)]. As a

[↓ PDF](#)

mask than when not wearing one. From 30 l/min to 60 l/min, an increasing flow rate persistently enhances the nasal deposition without a mask, while the nasal deposition with a mask shows a much lower sensitivity to the flow rate variation [Figs. 8(c) and 12(a)]. Reminding about the relatively constant nasal DF for different particle sizes at 30 l/min [Fig. 8(a)], the nasal DF increases slightly with particle size at 45 l/min and at a faster pace at 60 l/min; however, both are substantially slower than that without a mask [Fig. 13(a)]. Considering the larynx deposition, the DF peaked at 7 μm -10 μm with a mask and at 15 μm without a mask for all flow rates considered (except for 15 l/min). With a 65%-filtration mask, fewer particles deposited in the larynx for all particle sizes (1 μm -20 μm) and flow rates (15 l/min-60 l/min) considered in this study.



FIG. 13. Comparison of the regional airway dosimetry without vs with a mask (after correction) in the (a) nose and (b) larynx at different inhalation flow rates (15 l/min, 45 l/min, 60 l/min).

[↓ PPT](#) | [High-resolution](#)

[↓](#) PDF

particle deposition in the nose and larynx is shown in Figs. 14(a) and 14(b), respectively. The inhalation flow rate was 30 l/min, and four particle sizes were considered ($1\text{ }\mu\text{m}$, $5\text{ }\mu\text{m}$, $10\text{ }\mu\text{m}$, and $20\text{ }\mu\text{m}$). Overall, the mask resistance exerted an insignificant impact on the nasal DF. Minimal DF was observed for the mask with the most heterogeneous resistance (i.e., 10-1-10, blue bar), while similar nasal DFs were predicted for the two homogeneous masks (1-1-1 and 10-10-10) despite a ten times difference in the resistance magnitude. More erratic patterns were found in the larynx deposition with varying mask resistances, with no regular trend detected in light of the mask resistance variation. This lack of regular trend may be partially attributed to the flow instabilities in the pharynx and larynx, where fluctuations in airflow and particle deposition can occur.

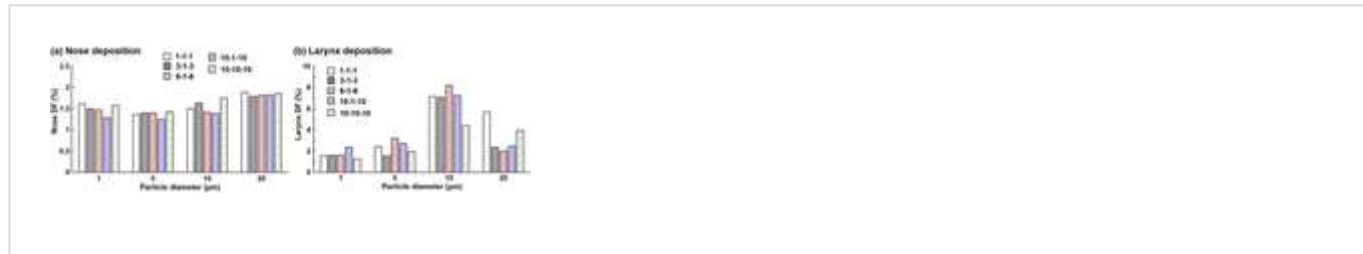


FIG. 14. Comparison of the regional airway dosimetry among different mask resistance matrices in the (a) nose and (b) larynx for particles of $1\text{ }\mu\text{m}$, $5\text{ }\mu\text{m}$, $10\text{ }\mu\text{m}$, and $20\text{ }\mu\text{m}$.

[PPT](#) | [High-resolution](#)

IV. DISCUSSION AND SUMMARY

[PDF](#)

been actively involved in elucidating transmission routes of SARS-CoV-2 viruses and devising ways to curb the transmission.^{40,41} Both optical visualization and numerical modeling have been undertaken to understand the respiratory flows and droplets from coughs and sneezes and the effectiveness of face-covering to curtail these droplets.^{1,18–20,42–45} In this study, we aimed at understanding the effect of mask-wearing on inspiratory airflows and their effects on the inhalability and deposition of ambient particles in the upper respiratory airways. A computational mask-face-airway model was developed that consisted of a three-layer surgical mask fitted on the face of an image-based head airway geometry. Factors that influence the inhalability into the nose/mouth and retention in the upper airway and lungs of ambient aerosols were examined, which include (a) with and without a mask, (b) mask filtration efficiency (0% vs 65%), (c) particle size (1 μm –20 μm), (d) inhalation flow rate (15 l/min–60 l/min), and (e) mask resistance (five matrices). We were interested in the dosimetry difference with and without a mask in different regions of the body (the face, upper airway, and lungs) and among the four sections of the upper airway (the nose, mouth, pharynx, and larynx). Mechanisms underlying these differences were explored, and their implications are discussed below.

Wearing a mask was found to notably change the airflow field and particle motions near the face. Due to the mask resistance, the speeds of both airflow and particles decreased in the otherwise respiration zones when no mask was worn; as a compensation, airflow and particles redistribute to regions other than these respiration zones of the mask because the same volume of air will be inhaled with or without a mask (Fig. 3). The overall



the nose, as well as their subsequent deposition in the upper airway. It is also found that the airflow speeds are higher near the folds or pleats of the mask, indicating the potential impacts of mask shape and morphological details on its protective efficacy.

The results of this study show that wearing a zero-filtration mask can lead to a higher deposition rate of particles smaller than $10 \mu\text{m}$ (i.e., PM10) in the upper airway for all flow rates (15 l/min–60 l/min) and mask resistance matrices considered. This seemingly counterintuitive observation may be attributed to the altered pressure and airflow fields caused by the mask, which further changes the inhalability of the particles and subsequent deposition in the upper airways. The overall lower speeds of the respirable particles after wearing a mask, as well as an increased area of respiration, can increase the chance of respirable particles to land on the face or being inhaled into the mouth and nose. This unexpected finding raises an alarm that wearing masks with very low filtration efficiencies may lead to a higher chance of deposition of ambient aerosols and thus can do more harm than protection. In this study, we assumed a 65% filtration efficiency of the mask, which is typical for a three-layer surgical mask, for all particle sizes. Luckily, the adjusted dosimetry of ambient aerosols is lower with a mask than without one for all particle sizes considered ($1 \mu\text{m}$ – $20 \mu\text{m}$) in the face, upper airway, and lungs. Considering that the nasal epithelium is one of three sites in the human body binding with the SARS-CoV-2 virus,^{46,47} wearing a 65%-filtration mask can reduce the nasal deposition (viral load) by half for $3 \mu\text{m}$ – $10 \mu\text{m}$ aerosols and by four to five times for $15\text{-}\mu\text{m}$ aerosols (Fig. 13).

without a mask calls for cautions in health risk assessment with face

coverings. The practice of estimating airway doses with a mask by simply scaling the doses without a mask can introduce significant errors.

Furthermore, current mask filtration efficiency (FE) testing, for instance, using TSI 8130, only provides an integrated FE value for polydisperse aerosols and does not differentiate FEs among particle sizes. It is well expected that the mask FE varies significantly with particle sizes. Even though this study adopted an identical FE (65%) for all particles considered, further studies with a mask are warranted to include the mask FEs that are specific to different particle sizes. Likewise, complementary experimental studies are needed to measure the particle-size-dependent FEs for different types of masks.

The nose has a unique role in this COVID-19 pandemic for several reasons. It is the first physical barrier of our body to keep ambient aerosols from getting into the respiratory tract; unlike the mouth, the downward nostrils can effectively prevent large particles from being inhaled due to their large inertia. The nasal mucus and immune cells constitute the second line of defense against invading viruses.⁴⁸ However, the nasal goblet secretory cells are also one of the three confirmed binding sites for COVID-19 viruses, where two necessary enzymes for cell invasion, ACE2 (angiotensin-converting enzyme 2) and TMPRSS2 (type II transmembrane serine protease), coexist.⁴⁷ This explains the usage of nasal swabs in COVID testing.⁴⁶ The other two sites with these two enzymes coexisting are the surface epithelial cells of the alveoli and the ileal absorptive cells in the small intestine.⁴⁷ In this study, we found that the protective efficacy of a mask for the nasal airway decreases at lower inhalation flow rates.

is even higher by wearing a 65% filtration mask than without a mask at all.

This situation is expected to worsen for flow rates lower than 15 l/min or wearing a mask with lower filtration efficiencies. After saying that, we also wish to emphasize that wearing a 65% filtration mask indeed reduces deposition of ambient aerosols larger than $3 \mu\text{m}$ on both the face and in all parts of the respiratory tract for all flow rates considered (15 l/min–60 l/min). Moreover, wearing a mask is highly effective in keeping large particles ($>10 \mu\text{m}$) from getting into the nostrils (i.e., particle inhalability), as illustrated in Figs. 8(c) and 13(a).

Limitations that may compromise the applicability of the results in this study include a perfect seal between the mask and the face, steady breathing, inhalation only, rigid airway walls, and an initial airborne aerosol profile of a spherical shape. It is well known that unlike N95, a disposable three-layer surgical mask does not fit tightly with the face;^{49,50} the fitting can become worse with physical activities or incorrect wearing practices.^{51,52} Air leakages through mask–face spaces can change the airflow and particle dynamics at different levels depending on the location and area of these opening spaces. Using a perfect mask–face seal here cuts the numerous possibilities of such open spaces short and intends to represent the optimal scenario in mask protection from ambient aerosols. However, imperfect mask–face sealing of varying degrees should be investigated to refine the assessment of mask protection efficiencies. Tidal breathing and compliant walls are the other two physiological factors determining respiratory aerodynamics, which further influence the trajectories, inhalability, and deposition of ambient aerosols.^{34,53} Furthermore, interpersonal transmissions of respiratory infectious

infected person, which produces a bolus of droplets that vary its shape and size distribution during its transportation through the air.^{42,54,55} In this sense, the spherical profile of monodisperse particles adopted in this study may not adequately represent the interpersonal transmissions. Moreover, the hygroscopic effects and electrostatic charges were excluded, both of which had been demonstrated to change the particle fates and behaviors.^{56–60} However, the computational model herein did take into account the most fundamental properties affecting a mask's performance, such as a realistic mask model with morphological details (folds) and experimentally determined properties (filtration efficiency and breathing resistance), an anatomically accurate face-airway geometry, and ambient aerosols are representative of COVID-19 virus-laden droplets.⁸ With the assumptions of a perfect mask-face interface, constant inhalation, non-moving walls, and monodisperse particles that greatly reduced numerical complexities, the results of this study provide a first-order approximation of mask performance in real life. Likewise, the computational model developed in this study can serve as a platform where more physiologically realistic factors can be evaluated.

In summary, the effects of wearing a three-layer surgical mask on airflow and aerosol dynamics were examined in a mask-face-airway model in comparison to without a mask. A better understanding of the factors involved in determining the dosimetry of ambient aerosols on the face and in the respiratory tract was obtained. Specific findings are as follows:

1. Wearing a mask significantly slows down inspiratory flows and extends respiration zones, which favors the inhalability of ambient aerosols into noses.



in the mask pleats.

3. Wearing a mask significantly reduces particle penetration into the lungs, regardless of the filtration efficiency of the mask. Wearing a 65%-filtration mask can reduce lung deposition by three folds for particles of size $1 \mu\text{m}$ - $10 \mu\text{m}$.
4. With a 65% mask filtration efficiency that is typical for a three-layer surgical mask, deposition is reduced by wearing a mask for all particle sizes considered, except $1 \mu\text{m}$ - $3 \mu\text{m}$, for which equivalent dosimetry in the upper airway was predicted.
5. Wearing a mask protects the upper airway (particularly the nose and larynx) best from particles larger than $10 \mu\text{m}$, while it protects the face and lungs best from particles less than $10 \mu\text{m}$ (PM10).
6. The mask protection of the nasal airway, whose goblet secretory cells are binding sites for SARS-CoV-2, decreases at lower inhalation flow rates (15 l/min or less).

ACKNOWLEDGMENTS

William Zouzas and Nathania Santoso at UMass Lowell Biomedical Engineering are gratefully acknowledged for reviewing this manuscript.

The authors report no conflicts of interest in this work.

DATA AVAILABILITY



corresponding author upon reasonable request.

REFERENCES

1. A. Agrawal and R. Bhardwaj, "Reducing chances of COVID-19 infection by a cough cloud in a closed space," *Phys. Fluids* **32**, 101704 (2020).
<https://doi.org/10.1063/5.0029186>, [Google Scholar](#), [Scitation](#), [ISI](#)

2. S. K. Das, J.-E. Alam, S. Plumari, and V. Greco, "Transmission of airborne virus through sneezed and coughed droplets," *Phys. Fluids* **32**, 097102 (2020). <https://doi.org/10.1063/5.0022859>, [Google Scholar](#), [Scitation](#), [ISI](#)

3. M. Gandhi and D. Havlir, "The time for universal masking of the public for coronavirus disease 2019 is now," *Open Forum Infect. Dis.* **7**, ofaa131 (2020). <https://doi.org/10.1093/ofid/ofaa131>, [Google Scholar](#), [Crossref](#)

4. S. E. Eikenberry, M. Mancuso, E. Iboi, T. Phan, K. Eikenberry, Y. Kuang, E. Kostelich, and A. B. Gumel, "To mask or not to mask: Modeling the potential for face mask use by the general public to curtail the COVID-19 pandemic," *Infect. Dis. Model.* **5**, 293–308 (2020).
<https://doi.org/10.1016/j.idm.2020.04.001>, [Google Scholar](#), [Crossref](#)

- respiratory cloth masks," ACS Nano **14**, 10742–10743 (2020).
<https://doi.org/10.1021/acsnano.0c04676>, Google Scholar, Crossref
-
6. R. J. Mason, "Pathogenesis of COVID-19 from a cell biology perspective," Eur. Respir. J. **55**, 2000607 (2020).
<https://doi.org/10.1183/13993003.00607-2020>, Google Scholar, Crossref
-
7. I.-M. Schaefer, R. F. Padera, I. H. Solomon, S. Kanjilal, M. M. Hammer, J. L. Hornick, and L. M. Sholl, "*In situ* detection of SARS-CoV-2 in lungs and airways of patients with COVID-19," Mod. Pathol. **33**, 2104–2114 (2020). <https://doi.org/10.1038/s41379-020-0595-z>, Google Scholar, Crossref
-
8. Y. Liu, Z. Ning, Y. Chen, M. Guo, Y. Liu, N. K. Gali, L. Sun, Y. Duan *et al.*, "Aerodynamic analysis of SARS-CoV-2 in two Wuhan hospitals," Nature **582**, 557–560 (2020). <https://doi.org/10.1038/s41586-020-2271-3>, Google Scholar, Crossref
-
9. J. Xi, M. Talaat, X. A. Si, and H. Kitaoka, "Micrometer aerosol deposition in normal and emphysematous subacinar models," Respir. Physiol. Neurobiol. **283**, 103556 (2021).
<https://doi.org/10.1016/j.resp.2020.103556>, Google Scholar, Crossref
-
10. I. Frerking, A. Günther, W. Seeger, and U. Pison, "Pulmonary

Intensive Care Med. 27, 1699–1717 (2001).

<https://doi.org/10.1007/s00134-001-1121-5>, Google Scholar, Crossref

11. M. Tadic, C. Cuspidi, G. Mancia, R. Dell'Oro, and G. Grassi, “COVID-19, hypertension and cardiovascular diseases: Should we change the therapy?,” Pharmacol. Res. 158, 104906 (2020).

<https://doi.org/10.1016/j.phrs.2020.104906>, Google Scholar, Crossref

12. I. Schröder, “COVID-19: A risk assessment perspective,” J. Chem. Health Saf. 27, 160–169 (2020).

<https://doi.org/10.1021/acs.chas.0c00035>, Google Scholar, Crossref

13. J. M. Leung, C. X. Yang, A. Tam, T. Shaipanich, T.-L. Hackett, G. K. Singhera, D. R. Dorscheid, and D. D. Sin, “ACE-2 expression in the small airway epithelia of smokers and COPD patients: Implications for COVID-19,” Eur. Respir. J. 55, 2000688 (2020).

<https://doi.org/10.1183/13993003.00688-2020>, Google Scholar, Crossref

14. A. C. Paulo, M. Correia-Neves, T. Domingos, A. G. Murta, and J. Pedrosa, “Influenza infectious dose may explain the high mortality of the second and third wave of 1918–1919 influenza pandemic,” PLoS One 5, e11655 (2010). <https://doi.org/10.1371/journal.pone.0011655>,

[Google Scholar](#), [Crossref](#)

<https://doi.org/10.1155/2014/859090>, [Google Scholar](#), [Crossref](#)

16. S. Pfefferle, T. Guenther, R. Kobbe, M. Czech-Sioli, D. Noerz, R. Santer, J. Oh, S. Kluge *et al.*, “Low and high infection dose transmission of SARS-CoV-2 in the first COVID-19 clusters in Northern Germany,” [MedRxiv:2020.2006.2011.20127332](https://doi.org/2020.2006.2011.20127332) (2020). [Google Scholar](#)
17. T. Watanabe, T. A. Bartrand, M. H. Weir, T. Omura, and C. N. Haas, “Development of a dose-response model for SARS coronavirus,” *Risk Anal.* **30**, 1129–1138 (2010).
<https://doi.org/10.1111/j.1539-6924.2010.01427.x>, [Google Scholar](#), [Crossref](#)
18. P. P. Simha and P. S. M. Rao, “Universal trends in human cough airflows at large distances,” *Phys. Fluids* **32**, 081905 (2020).
<https://doi.org/10.1063/5.0021666>, [Google Scholar](#), [Scitation](#)
19. S. Verma, M. Dhanak, and J. Frankenfield, “Visualizing the effectiveness of face masks in obstructing respiratory jets,” *Phys. Fluids* **32**, 061708 (2020). <https://doi.org/10.1063/5.0016018>, [Google Scholar](#), [Scitation](#), [ISI](#)
20. S. Verma, M. Dhanak, and J. Frankenfield, “Visualizing droplet dispersal for face shields and masks with exhalation valves,” *Phys. Fluids* **32**, 091701 (2020). <https://doi.org/10.1063/5.0022968>,

21. J. W. Tang, T. J. Liebner, B. A. Craven, and G. S. Settles, “A schlieren optical study of the human cough with and without wearing masks for aerosol infection control,” *J. R. Soc., Interface* **6**(Suppl 6), S727–S736 (2009). <https://doi.org/10.1098/rsif.2009.0295.focus>, [Google Scholar](#), [Crossref](#)
-
22. S. Asadi, C. D. Cappa, S. Barreda, A. S. Wexler, N. M. Bouvier, and W. D. Ristenpart, “Efficacy of masks and face coverings in controlling outward aerosol particle emission from expiratory activities,” *Sci. Rep.* **10**, 15665 (2020). <https://doi.org/10.1038/s41598-020-72798-7>, [Google Scholar](#), [Crossref](#)
-
23. T. Dbouk and D. Drikakis, “On respiratory droplets and face masks,” *Phys. Fluids* **32**, 063303 (2020). <https://doi.org/10.1063/5.0015044>, [Google Scholar](#), [Scitation](#), [ISI](#)
-
24. J. Xi, J. Kim, X. A. Si, R. A. Corley, and Y. Zhou, “Modeling of inertial deposition in scaled models of rat and human nasal airways: Towards *in vitro* regional dosimetry in small animals,” *J. Aerosol Sci.* **99**, 78–93 (2016). <https://doi.org/10.1016/j.jaerosci.2016.01.013>, [Google Scholar](#), [Crossref](#)
-
25. J. Xi and P. W. Longest, “Numerical predictions of submicrometer aerosol deposition in the nasal cavity using a novel drift flux approach,” *Int. J. Heat Mass Transfer* **51**, 5562–5577 (2008)

[Google Scholar](#), [Crossref](#)

26. J. Xi and P. Longest, "Effects of oral airway geometry characteristics on the diffusional deposition of inhaled nanoparticles," *J. Biomech. Eng.* **130**, 011008 (2008). <https://doi.org/10.1115/1.2838039>,

[Google Scholar](#), [Crossref](#)

27. Y.-S. Cheng, Y. Zhou, and B. T. Chen, "Particle deposition in a cast of human oral airways," *Aerosol Sci. Technol.* **31**, 286–300 (1999).

<https://doi.org/10.1080/027868299304165>, [Google Scholar](#), [Crossref](#)

28. J. Xi and P. W. Longest, "Transport and deposition of micro-aerosols in realistic and simplified models of the oral airway," *Ann. Biomed. Eng.* **35**, 560–581 (2007). <https://doi.org/10.1007/s10439-006-9245-y>,

[Google Scholar](#), [Crossref](#)

29. D. C. Wilcox, "Formulation of the k-w turbulence model revisited," *AIAA J.* **46**, 2823–2838 (2008). <https://doi.org/10.2514/1.36541>,

[Google Scholar](#), [Crossref](#)

30. J. Xi, X. Si, J. Kim, G. Su, and H. Dong, "Modeling the pharyngeal anatomical effects on breathing resistance and aerodynamically generated sound," *Med. Biol. Eng. Comput.* **52**, 567–577 (2014).

<https://doi.org/10.1007/s11517-014-1160-z>, [Google Scholar](#), [Crossref](#)

expiratory airflow and submicrometer particle deposition in human extrathoracic airways," *Open J. Fluid Dyn.* **3**, 286–301 (2013).
<https://doi.org/10.4236/ojfd.2013.34036>, [Google Scholar](#), [Crossref](#)

32. P. W. Longest and J. Xi, "Effectiveness of direct Lagrangian tracking models for simulating nanoparticle deposition in the upper airways," *Aerosol Sci. Technol.* **41**, 380–397 (2007).

<https://doi.org/10.1080/02786820701203223>, [Google Scholar](#), [Crossref](#)

33. J. Xi, J. E. Yuan, M. Yang, X. Si, Y. Zhou, and Y.-S. Cheng, "Parametric study on mouth-throat geometrical factors on deposition of orally inhaled aerosols," *J. Aerosol Sci.* **99**, 94–106 (2016).

<https://doi.org/10.1016/j.jaerosci.2016.01.014>, [Google Scholar](#), [Crossref](#)

34. J. Kim, J. Xi, X. Si, A. Berlinski, and W. C. Su, "Hood nebulization: Effects of head direction and breathing mode on particle inhalability and deposition in a 7-month-old infant model," *J. Aerosol Med. Pulm. Drug Delivery* **27**, 209–218 (2014).

<https://doi.org/10.1089/jamp.2013.1051>, [Google Scholar](#), [Crossref](#)

35. Z. Li, C. Kleinstreuer, and Z. Zhang, "Simulation of airflow fields and microparticle deposition in realistic human lung airway models. Part II: Particle transport and deposition," *Eur. J. Mech.: B/Fluids* **26**, 650–668 (2007). <https://doi.org/10.1016/j.euromechflu.2007.02.004>

-
36. Z. Liu, D. Yu, Y. Ge, L. Wang, J. Zhang, H. Li, F. Liu, and Z. Zhai, “Understanding the factors involved in determining the bioburdens of surgical masks,” *Ann. Transl. Med.* **7**, 754 (2019).
<https://doi.org/10.21037/atm.2019.11.91>, [Google Scholar](#), [Crossref](#)
-
37. E. J. Sinkule, J. B. Powell, and F. L. Goss, “Evaluation of N95 respirator use with a surgical mask cover: Effects on breathing resistance and inhaled carbon dioxide,” *Ann. Occup. Hyg.* **57**, 384–398 (2013).
<https://doi.org/10.1093/annhyg/mes068>, [Google Scholar](#), [Crossref](#)
-
38. J. Xi, Z. Zhang, and X. Si, “Improving intranasal delivery of neurological nanomedicine to the olfactory region using magnetophoretic guidance of microsphere carriers,” *Int. J. Nanomed.* **10**, 1211–1222 (2015). <https://doi.org/10.2147/ijn.s77520>, [Google Scholar](#), [Crossref](#)
-
39. J. Xi, J. Kim, and X. Si, “Effects of nostril orientation on airflow dynamics, heat exchange, and particle depositions in human noses,” *Eur. J. Mech.: B/Fluids* **55**, 215–228 (2015).
<https://doi.org/10.1016/j.euromechflu.2015.08.014>, [Google Scholar](#), [Crossref](#)
-
40. Y.-Y. Li, J.-X. Wang, and X. Chen, “Can a toilet promote virus transmission? From a fluid dynamics perspective,” *Phys. Fluids* **32**,

Scitation, ISI

-
41. J.-X. Wang, Y.-Y. Li, X.-D. Liu, and X. Cao, "Virus transmission from urinals," *Phys. Fluids* **32**, 081703 (2020).

<https://doi.org/10.1063/5.0021450>, [Google Scholar](#), [Scitation](#), [ISI](#)

-
42. M.-R. Pendar and J. C. Páscoa, "Numerical modeling of the distribution of virus carrying saliva droplets during sneeze and cough," *Phys. Fluids* **32**, 083305 (2020).

<https://doi.org/10.1063/5.0018432>, [Google Scholar](#), [Scitation](#), [ISI](#)

-
43. S. H. Smith, G. A. Somsen, C. van Rijn, S. Kooij, L. van der Hoek, R. A. Bem, and D. Bonn, "Aerosol persistence in relation to possible transmission of SARS-CoV-2," *Phys. Fluids* **32**, 107108 (2020).

<https://doi.org/10.1063/5.0027844>, [Google Scholar](#), [Scitation](#), [ISI](#)

-
44. R. Mittal, C. Meneveau, and W. Wu, "A mathematical framework for estimating risk of airborne transmission of COVID-19 with application to face mask use and social distancing," *Phys. Fluids* **32**, 101903 (2020).

<https://doi.org/10.1063/5.0025476>, [Google Scholar](#), [Scitation](#), [ISI](#)

-
45. T. Dbouk and D. Drikakis, "On coughing and airborne droplet transmission to humans," *Phys. Fluids* **32**, 053310 (2020).

<https://doi.org/10.1063/5.0011960>, [Google Scholar](#), [Scitation](#), [ISI](#)

highly expressed in nasal epithelial cells together with innate immune genes,” Nat. Med. **26**, 681–687 (2020).

<https://doi.org/10.1038/s41591-020-0868-6>, [Google Scholar](#),

[Crossref](#)

47. C. G. K. Ziegler, S. J. Allon, S. K. Nyquist, I. M. Mbano, V. N. Miao, C. N. Tzouanas, Y. Cao, A. S. Yousif *et al.*, “SARS-CoV-2 receptor ACE2 is an interferon-stimulated gene in human airway epithelial cells and is detected in specific cell subsets across tissues,” Cell **181**, 1016–1035 (2020). <https://doi.org/10.1016/j.cell.2020.04.035>, [Google Scholar](#), [Crossref](#)

48. R. L. Chua, S. Lukassen, S. Trump, B. P. Hennig, D. Wendisch, F. Pott, O. Debnath, L. Thürmann *et al.*, “COVID-19 severity correlates with airway epithelium-immune cell interactions identified by single-cell analysis,” Nat. Biotechnol. **38**, 970–979 (2020).
<https://doi.org/10.1038/s41587-020-0602-4>, [Google Scholar](#), [Crossref](#)

49. P. Bradford Smith, G. Agostini, and J. C. Mitchell, “A scoping review of surgical masks and N95 filtering facepiece respirators: Learning from the past to guide the future of dentistry,” Saf. Sci. **131**, 104920 (2020).
<https://doi.org/10.1016/j.ssci.2020.104920>, [Google Scholar](#), [Crossref](#)

50. J. D. Smith, C. C. MacDougall, J. Johnstone, R. A. Copes, B. Schwartz,

masks in protecting health care workers from acute respiratory infection: A systematic review and meta-analysis," *Can. Med. Assoc. J.* **188**, 567–574 (2016). <https://doi.org/10.1503/cmaj.150835>, [Google Scholar](#), [Crossref](#)

51. A. C. K. Lai, C. K. M. Poon, and A. C. T. Cheung, "Effectiveness of facemasks to reduce exposure hazards for airborne infections among general populations," *J. R. Soc., Interface* **9**, 938–948 (2012).
<https://doi.org/10.1098/rsif.2011.0537>, [Google Scholar](#), [Crossref](#)
52. L. Y.-K. Lee, E. P.-W. Lam, C.-K. Chan, S.-Y. Chan, M.-K. Chiu, W.-H. Chong, K.-W. Chu, M.-S. Hon *et al.*, "Practice and technique of using face mask amongst adults in the community: A cross-sectional descriptive study," *BMC Public Health* **20**, 948 (2020).
<https://doi.org/10.1186/s12889-020-09087-5>, [Google Scholar](#), [Crossref](#)
53. K. Talaat and J. Xi, "Computational modeling of aerosol transport, dispersion, and deposition in rhythmically expanding and contracting terminal alveoli," *J. Aerosol Sci.* **112**, 19–33 (2017).
<https://doi.org/10.1016/j.jaerosci.2017.07.004>, [Google Scholar](#), [Crossref](#)
54. C. J. Worby and H.-H. Chang, "Face mask use in the general population and optimal resource allocation during the COVID-19 pandemic," *Nat. Commun.* **11**, 4049 (2020).



[Crossref](#)

-
55. M. Jayaweera, H. Perera, B. Gunawardana, and J. Manatunge, “Transmission of COVID-19 virus by droplets and aerosols: A critical review on the unresolved dichotomy,” *Environ. Res.* **188**, 109819 (2020). <https://doi.org/10.1016/j.envres.2020.109819>, [Google Scholar](#), [Crossref](#)
-
56. J. W. Kim, J. Xi, and X. A. Si, “Dynamic growth and deposition of hygroscopic aerosols in the nasal airway of a 5-year-old child,” *Int. J. Numer. Methods Biomed. Eng.* **29**, 17–39 (2013). <https://doi.org/10.1002/cnm.2490>, [Google Scholar](#), [Crossref](#)
-
57. J. Xi, J. Kim, X. A. Si, and Y. Zhou, “Hygroscopic aerosol deposition in the human upper respiratory tract under various thermo-humidity conditions,” *J. Environ. Sci. Health, Part A* **48**, 1790–1805 (2013). <https://doi.org/10.1080/10934529.2013.823333>, [Google Scholar](#), [Crossref](#)
-
58. Y. Feng, T. Marchal, T. Sperry, and H. Yi, “Influence of wind and relative humidity on the social distancing effectiveness to prevent COVID-19 airborne transmission: A numerical study,” *J. Aerosol Sci.* **147**, 105585 (2020). <https://doi.org/10.1016/j.jaerosci.2020.105585>, [Google Scholar](#), [Crossref](#)
-

Pharmaceutics **6**, 26–35 (2013).

<https://doi.org/10.3390/pharmaceutics6010026>, Google Scholar, Crossref

-
60. J. Xi, X. A. Si, and R. Gaide, “Electrophoretic particle guidance significantly enhances olfactory drug delivery: A feasibility study,” PLoS One **9**, e86593 (2014).

<https://doi.org/10.1371/journal.pone.0086593>, Google Scholar, Crossref

Published under license by AIP Publishing.



Resources

AUTHOR

LIBRARIAN

ADVERTISER

 PDF

General Information

ABOUT

CONTACT

HELP

PRIVACY POLICY

TERMS OF USE

FOLLOW AIP PUBLISHING:



Website © 2020 AIP Publishing LLC.

Article copyright remains as
specified within the article.

Scitation

